RESTRICTED

NOV 30 1944

NATIONAL ADVISORY COMMITTEE FOR AERONAUTICS

TECHNICAL NOTE

No. 954

PERFORMANCE TESTS OF WIRE STRAIN GAGES

I - CALIBRATION FACTORS IN TENSION

By William R. Campbell
National Bureau of Standards

Washington
November 1944

CLASSIFIED DOCUMENT

This document contains classified information affecting the National Defense of the United States within the meaning of the Espionage Act, USC 50:31 and 32. Its transmission or the revelation of its contents in any manner to an unauthorized person is prohibited by law. Information so classified may be imparted only to persons in the military and naval Services of the United States, appropriate civilian officers and employees of the Federal Government who have a legitimate interest therein, and to United States citizens of known loyalty and discretion who of necessity must be informed thereof.

RESTRICTED

NATIONAL ADVISORY COMMITTEE FOR AERONAUTICS

TECHNICAL NOTE NO. 954

PERFORMANCE TESTS OF WIRE STRAIN GAGES

I - CALIBRATION FACTORS IN TENSION

By William R. Campbell

SUMMARY

Results of calibrations in axial tension over the strain range 0 to 0.0024 are presented for 15 types of single element multistrand wire strain gages. The majority of gages showed significant differences between the calibration factors for strain increasing and strain decreasing. Zero shift and nonlinearity between gage output and strain were present in nearly all gages. Improvement in gage performance after preloading was apparent in most cases. The maximum difference between the calibration factors for the gages of a given type and the average factor for that type ranged from 1 percent or less for the gages of types B, F, I, M, N, and J to more than 7 percent for the gage of types G and H.

INTRODUCTION

This report covers one phase of a series of performance tests on wire strain gages of types currently used in large numbers to measure stresses in aircraft structures. The purpose of the tests is to make available information on the properties, accuracy, and limitations of various multistrand, single element gages.

The performance test program has been divided into several phases the results of which are to be reported individually. The present paper reports on the first phase, calibrations under axial tension at strains between 0 and 0.0024.

This investigation, conducted at the National Bureau of Standards, was sponsored by and conducted with the financial assistance of the National Advisory Committee for Aeronautics.

The author desires to acknowledge the cooperation of the NACA Ames Aeronautical Laboratory, the Baldwin Locomotive Works, the Boeing Aircraft Company, the Chrysler Corporation, the Consolidated Vultee Aircraft Corporation, the Douglas Aircraft Company, the Lockheed Aircraft Corporation, North American Aviation Incorporated, and Northrop Aircraft Incorporated in submitting test gages. The ratio set used in calibrating the wire strain gages was designed for these tests by Dr. Frank Wenner. The author is indebted to Dr. Wenner and to members of the Engineering Mechanics Section of the National Bureau of Standards for suggestions and assistance on the test program.

APPARATUS AND METHOD

Description of Strain Gages

Six aircraft companies, the NACA Ames Aeronautical Laboratory, the Baldwin Locomotive Works, and the Chrysler Corporation contributed a total of 120 gages of 15 different types including gages which are commercially available and gages which are manufactured for use only in the laboratories of the maker. An attempt was made to include all types of wire strain gages which are used in large numbers for measuring strains on aircraft structures on tho ground and in flight. No attempt was made to include gages for measuring strains at high temperature, gages having an impedance large compared to 100 ohms, gages with a gage length small compared to 1 inch, and other gages of special types.

Each gage tested was identified by a letter A, B, . . ., O indicating the type, followed by a number 1, 2, . . ., 8 indicating the order in which it was tested. Table 1 gives a description of the gages. Figures 1 and 2 show the gages attached to test strips for calibration.

Attachment of Gages

Each maker was asked to attach eight gages of each type of his make to test strips furnished by the National Bureau of Standards, using his own preferred method of attachment. Four gages were attached to each of two 30- by 1- by 0.125-inch 24S-T aluminum-alloy calibration strips as shown in figure 3. After attachment of gages, the strips were returned to the Bureau for gage calibrations.

Each maker was asked not to apply any loads to the strips, so that all gages would be received at the Bureau in a new condition.

Calibrations and Calibrating Equipment

The gages were calibrated by measuring relative changes in resistance $\Delta R/R$ corresponding to known changes in strain ϵ. The calibration factor was defined by

$$K = \frac{\Delta R}{R} \frac{1}{\epsilon} \tag{1}$$

The relative changes in resistance $\Delta R/R$ were measured for strains between 4×10^{-4} and 24×10^{-4}. The lower limit of 4×10^{-4} was chosen as sufficient to aline the test strip in the testing machine. The upper limit of 24×10^{-4} was chosen to be inside the linear portion of the stress-strain curve of the test-strip material.

Calibration factors K were determined as the slope of a straight line fitted by least squares to a plot of $\Delta R/R$ against ϵ.

Strain Measurements

The calibrating strain applied to each wire gage was measured with a Tuckerman optical strain gage (references 1 and 2) having a 0.4-inch lozenge and a 3-inch gage length (fig. 3). The same Tuckerman gage was used for each of the 120 wire gages calibrated.

Resistance Measurements

The percentage change in resistance of each test gage during calibration was measured with a Wenner-type, direct-reading ratio set, in a direct-current Wheatstone bridge using a high-sensitivity moving-coil galvanometer as a null indicator.

A circuit diagram of the Wheatstone bridge is shown in figure 4. The arm R of the bridge represents the test gage and the arm T the temperature-compensating gage. The arms A and B represent the two arms of the ratio set. The ratio set is shown in figure 5.

The A-arm of the bridge has a nominal resistance of 100 ohms and is of the adjustable, direct-reading type discussed in reference 3. It consists of shunted-resistance sections which are adjustable by means of dial switches in steps of 0.0001, 0.001, 0.01, and 0.1 ohm. The A-arm has a resistance of 100 ohms when the reading of the dial switches is approximately 5555, and may be varied from 0.5 percent below to 0.5 percent above its nominal resistance.

The B-arm is similar in construction to the A-arm. It also has a nominal resistance of 100 ohms and is equipped with two dial switches for varying the resistance of the arm from 2 percent below to 2 percent above its nominal value in steps of 0.04 and 0.4 ohm. A dial switch reading of 55 sets the B-arm at its nominal value.

The ratio set (fig. 5) is provided with terminals for the R and T arms of the bridge, the battery, and the galvanometer, and includes adjustable series and parallel resistances for varying the damping of the galvanometer.

The relative change in resistance $\Delta R/R$ of the test gage due to a change in strain ϵ was measured by the Wheatstone bridge of figure 4 by balancing the bridge before the application of strain and then balancing again after the application of strain. The condition of balance before the application of strain is given by

$$(R + r)B = (A + a)T \tag{2}$$

where

r resistance of cable connecting test gage to ratio set, that is, total resistance from b to c minus resistance of test gage ($r = 0.0345$ ohm in present setup)

R initial resistance of test gage

A resistance of A-arm with dials set at 5555 ($A = 100$ ohms)

a resistance added to A-arm by change in dial setting from 5555

T resistance between a and b

B resistance between a and d

The condition of balance after the application of strain is

$$(R + r + \Delta R)B = (A + a + \Delta A)T \tag{3}$$

where

ΔA change in resistance of arm A to balance change in resistance ΔR of test gage

Eliminating B and T from equations (2) and (3) gives

$$\frac{\Delta R}{R} = \frac{\Delta A}{A + a}\left(1 + \frac{r}{R}\right) \tag{4}$$

The resistance a, added to the A-arm, was adjusted to make

$$a = A\frac{r}{R} \tag{5}$$

so that equation (4) reduced to the convenient form

$$\frac{\Delta R}{R} = \frac{\Delta A}{A} \tag{6}$$

that is, the percentage change in resistance of the test gage is equal to the percentage change in resistance of the A-arm of the ratio set. The adjustment (equation (5)) was easily made at the beginning of each calibration by substituting in equation (5) the measured value of R for the test gage and the fixed values of A and r.

The maximum permissible voltage drop across the test gage specified by the makers of the gages was equal to or greater than 1 volt. However, the voltage drop was limited in the calibrations to 0.75 volt, as this was found to provide ample bridge sensitivity.

The combined sensitivity of the bridge and galvanometer (fig. 6) was such that at a scale distance of 2 meters, with the galvanometer critically damped, a lack of balance of 1 part in 1 million produced a scale deflection of approximately 2 millimeters upon reversal of the battery current.

TEST PROCEDURE

The same procedure was followed in calibrating all gages.

One of the test strips upon which four gages were attached was mounted in 1-inch Templin grips in a 60,000-pound testing machine as shown in figure 7. A load of 500 pounds was applied to aline the strip and to facilitate the attachment of the Tuckerman strain gage A. The Tuckerman gage was mounted on the strip so as to span the wire gage and contact the strip at points equidistant from the transverse center line of the strain-sensitive element (figs. 3 and 7). On the opposite side of the strip a dummy gage B (having a gage length equal to that of the Tuckerman gage) was mounted for the purpose of balancing the lozenge and knife-edge reactions of the Tuckerman gage. Spacing jigs were used to locate the Tuckerman gage in the center of the strip and parallel to its edge.

The other strip C, upon which were also attached four wire gages, was clamped in an improvised grip (fig. 7) attached to the machine head so as to hang free beside the strip under load. One of the wire gages on this unloaded strip was used as the compensating gage (bridge arm T) during the calibrations of the four gages on the loaded strip. A 2-inch Tuckerman gage D was attached to the unloaded strip. This gage was read at the beginning and the end of each calibration to determine the magnitude of errors in the calibrating strain caused by differential expansion between the Tuckerman gage A and the test strip resulting from the slow change in temperature in the insulated test room. As will be shown later, errors from this source were small and, consequently, were neglected.

With the dial switches in the A-arm of the bridge set to a reading of (5555 + a) where a satisfied the condition (equation (5)), the B-arm dial switches were set to within 0.02 percent of balance. The load was varied (by not more than 100 lb) to a position where a small increase in load would balance the bridge. The load was slowly increased and the strain was read at the moment of balance. The actual calibration from then on consisted in setting known resistance changes on the A-arm dial switches, increasing the load to the point at which the wire-gage output rebalanced the bridge, and measuring the strain at the instant of balance with the Tuckerman gage. The dial settings in the A-arm were changed by equal increments, usually 0.03 percent, to facilitate computation. The load was increased until the strain at the gage was $24 \times 10^{-4} \pm 0.7 \times 10^{-4}$ and then was decreased and strains were measured at the same A-arm settings as for increasing load.

After the first gage on the strip was calibrated, the Tuckerman gage was removed and attached so as to span the second wire gage, and the strip was reloaded for another calibration. After the fourth gage was calibrated, the loaded and unloaded strips were interchanged, and calibrations were made on the second set of four gages using a gage of the first set for temperature compensation.

ACCURACY

The accuracy of the calibration factors depends according to equation (1) on the accuracy in the measurement of percentage change in resistance and the accuracy in the measurement of change in strain.

The measurement of change in resistance may be in error due to deviation of the resistance in the ratio set from the values indicated by the dials and to the presence of resistance in the gage-to-bridge cable.

The ratio set was calibrated by the Resistance Measurements Section of the National Bureau of Standards. It was found to measure changes in resistance with an accuracy of 0.1 percent over a range equal to the total range provided by the dial switches and over a range equal to one-tenth of the total range. It was found to be accurate to 1 part in 1 million on the 100-ohm resistance of arms A and B (0.0001 ohm) for changes in resistance less than one-tenth of the total range.

Correction for the effect of cable resistance was made by adjusting the initial setting of the A-arm of the ratio set to satisfy equation (5). With this correction the error from this source was estimated to be of a smaller order than 0.1 percent.

On combining the two effects and noting that the sensitivity of the galvanometer was sufficient to measure changes in resistance of 1 part in 1 million, it was estimated that the total error in calibration factor due to inaccuracy in the measurement of resistance did not exceed 0.1 percent.

The error in calibration factor due to inaccuracy in the measurement of strain acting along the strain-sensitive element of the wire gage is more difficult to estimate.

The Tuckerman strain gage spanning the wire gage was calibrated with an interferometer over the portion of the reticulo scale used during the tests of the wire gages. Three calibrations were made on the Tuckerman gage; the first one before tests, the second after tests on seven types of gages, and the third after completion of tests. No single calibration factor differed from the median or average factor by more than 0.083 percent. No single observation differed from the calculated autocollimator reading by more than 0.011 division, corresponding to a strain of 1.4×10^{-6} for the gage length and lozenge combination used. The error in calibration factor from this source would be, therefore, of the order of 0.1 percent if the strain-sensitive grid of the wire gage occupied the exact gage length of the Tuckerman gage and if both gage and strip were at exactly the same temperature, thus eliminating differential expansion as a source of error.

Actually the strain-sensitive grid was less than one-half as long as the gage length of the Tuckerman gage. Consequently, there may be small errors due to nonlinear variations in thickness or in bending strain along the strip. A strain survey of a test strip loaded as in the calibrations indicated that these nonlinear effects would introduce errors the order of magnitude of which did not exceed 0.2 percent.

The error due to differential expansion of the Tuckerman gage and the strip was minimized by housing the testing machine and apparatus in an insulated room. The variation in ambient temperature at the test strip did not exceed 0.3° C during the calibration of 97 percent of the gages; it was as much as 0.6° C for only one calibration. Measurements with a Tuckerman gage on a test strip indicated strains of the order of 10^{-5} per degree centigrade due to differential expansion. An interval of 15 minutes was allowed before each calibration for the Tuckerman gage to come to ambient temperature after handling. With the above-mentioned precautions it was estimated that the error in calibration factor due to temperature variations did not exceed 0.3 percent.

When the errors in both measurements of resistance and of strain were combined, it was estimated that the total error in calibration factor did not exceed ±0.5 percent.

Examination of the consistency of the data obtained leads to an estimated error in calibration factor of the order of ±0.3 percent.

RESULTS

Gage resistances, and calibration factors defined by equation (1) are given in table 2. Two calibration factors are given for each gage tested: K_u for increasing strain, and K_d for decreasing strain. Each of these calibration factors was determined as the slope of a line fitted by least squares to a plot of $\Delta R/R$ against ϵ for strain increasing and strain decreasing, respectively.

The experimental data are presented in the form of strain-deviation curves to magnify the deviations from the linear relationship given by equation (1). The method of obtaining the strain-deviation curves is illustrated by the hypothetical curves in figure 8. The curves on the left represent calibration data for two gages, one (A, B) with an output greater than that corresponding to the average factor K_m for the 16 calibrations on gages of this type (dotted line) and one (C, D) with an output less than that corresponding to the average. In the curves on the right the same data are plotted against strain deviation $\epsilon - 1/K_m(\Delta R/R)$ from the average line with slope K_m. This method of plotting brings out clearly the nature of the deviation from nominal linear behavior. Hysteresis is indicated by the width of the loop, zero shift by the opening of the loop at the bottom, deviation in calibration factor from the nominal value K_m by the tilt relative to the vertical axis.

Strain-deviation curves for the test gages are shown in figures 9 to 23. Gage numbers, appearing above each curve, represent the order in which the gages were calibrated. As noted in table 2, gages 1 and 5 were tested without preloading, gages 2 and 6 with one cycle of preloading, gages 3 and 7 with two cycles, and gages 4 and 8 with three cycles.

Table 3 shows the maximum spread in strain deviation obtained from figures 9 to 23 as the width of vertical band just enclosing all points. The gage types are arranged in order of increasing spread.

Figures 24 to 26 show the calibration factors for the individual gages plotted against gage number and preloads.

DISCUSSION

The calibrations have shown several performance characteristics which in varying degrees were common to all the gages tested. Examination of the deviation curves of figures 9 to 23 shows that in every calibration the curve for strain decreasing from the maximum value deviated from the curve for strain increasing by an amount greater than the experimental scatter of measurements. Owing to this deviation there was a zero shift after a cycle of loading which ranged from 0 to more than 100×10^{-6}. The linearity was generally better for decreasing strain than for increasing strain. There was a general improvement in performance after preloading; the deviation was consistently smaller for gages 4 and 8 with three cycles of preloading than for gages 1 and 5 with no preloading.

The last point is brought out by an examination of calibration factors in figures 24 to 26. The calibration factors of gages 1 and 5 were from 9 percent below to 3 percent above the mean value K_m; while those for gages 4 and 8 were only 1 percent below to 4 percent above K_m.

Figures 24 to 26 also show that some types of gages had a much smaller scatter in calibration factor than other types. The maximum difference between the calibration factors for the gages of a given type and the average factor for that type ranged from 1 percent or less for gages of types B, F, I, M, N, and J to more than 7 percent for gages of types G and H.

Table 3 shows that the spread in strain deviation for the first four types of gages differed less than 40 percent from the minimum spread of 28×10^{-6} for gages I; while that of the last four types was more than six times as great.

National Bureau of Standards,
Washington, D. C., June 1944.

REFERENCES

1. Tuckerman, L. B.: Optical Strain Gages and Extensometers. Proc. A.S.T.M., vol. 23, 1923, pt. II, p. 602-610.

2. Wilson, B. L.: Characteristics of the Tuckerman Strain Gage. A.S.T.M. Preprint 94, 1944. Paper presented at the Annual Meeting of the A.S.T.M., June 26 to 30, 1944.

3. Mueller, E. F., and Wonner, Frank: The Waidner-Wolff and Other Adjustable Electrical Resistance Elements. Res. Paper 842, Nat. Bur. of Standards Jour. Res., vol. 15, 1935, p. 477.

Table 1. Description of Gages

Gage type	Nominal Dimensions length	Nominal Dimensions width	Approximate length of grid	Wire material	Cement	Type of winding	Nominal Resistance
	in.	in.	in.				ohms
A	0.87	0.31	0.62	Advance	Duco	Grid	120
B	2.00	0.40	1.00	"	General Service	"	100
C	1.75	0.44	1.00	--	Duco	"	88
D	1.87	0.50	0.82	Cu-Ni	"	"	120
E	2.00	0.40	1.00	Advance	General Service	"	400
F	1.37	0.50	0.50	Cu-Ni	Duco	"	120
G	1.12	0.44	1.00	Chromel	"	"	120
H	1.80	0.30	1.00	--	"	"	49
I	1.75	0.37	0.82	Cu-Ni	"	"	120
J	2.00	0.37	1.12	Advance	Celluloid	"	300
K	2.00	0.25	1.25	"	Duco	"	50
L	0.75	0.31	0.31	--	"	"	120
M	0.75	0.31	0.25	Cu-Ni	"	Helical	120
N	2.12	0.50	1.06	Isoelastic	"	Grid	500
O	1.50	0.25	1.00	Advance	Celluloid	"	100

Table 2. Results of Tests.

Gage Type	Gage No.	Resistance R ohms	Calibration increasing strain K_u	Factors decreasing strain K_d	K_u/K_d	No of Preloads
A	1	116.7	1.994	2.020	0.987	0
	2	117.0	2.023	2.035	0.994	1
	3	116.9	1.995	2.001	0.997	2
	4	116.9	2.017	2.026	0.996	3
	5	115.9	2.020	2.036	0.992	0
	6	115.9	2.038	2.046	0.996	1
	7	115.9	2.051	2.049	1.001	2
	8	115.7	2.037	2.042	0.997	3
B	1	99.8	2.088	2.091	0.999	0
	2	99.8	2.065	2.072	0.996	1
	3	99.7	2.084	2.089	0.998	2
	4	99.8	2.089	2.092	0.998	3
	5	99.9	2.070	2.086	0.992	0
	6	99.8	2.087	2.090	0.999	1
	7	99.8	2.071	2.087	0.992	2
	8	99.8	2.080	2.086	0.997	3
C	1	87.8	2.008	2.038	0.985	0
	2	88.4	2.026	2.045	0.990	1
	3	88.0	2.052	2.053	1.000	2
	4	88.3	2.033	2.042	0.996	3
	5	88.0	2.013	2.048	0.983	0
	6	88.5	2.029	2.043	0.993	1
	7	88.9	2.023	2.025	0.999	2
	8	88.8	2.027	2.044	0.991	3
D	1	120.7	2.028	2.065	0.982	0
	2	120.5	2.044	2.060	0.992	1
	3	120.5	2.056	2.064	0.996	2
	4	120.5	2.064	2.070	0.997	3
	5	120.5	2.037	2.074	0.983	0
	6	120.4	2.054	2.060	0.997	1
	7	120.5	2.058	2.067	0.996	2
	8	120.5	2.060	2.070	0.995	3

Table 2. Results of Tests. (continued)

Gage Type	Gage No.	Resistance R ohms	Calibration increasing strain K_u	Factors decreasing strain K_d	K_u/K_d	No. of Preloads
E	1	398.7	2.098	2.123	0.988	0
	2	399.0	2.109	2.119	0.995	1
	3	398.9	2.065	2.076	0.995	2
	4*	398.8	--	--	--	3
	5	399.0	2.114	2.131	0.992	0
	6	398.9	2.058	2.074	0.992	1
	7	398.7	2.139	2.146	0.996	2
	8	398.8	2.101	2.110	0.996	3
F	1	120.5	2.026	2.046	0.990	0
	2	120.3	2.025	2.039	0.993	1
	3	120.3	2.049	2.055	0.997	2
	4	120.5	2.038	2.049	0.995	3
	5	120.3	2.009	2.030	0.990	0
	6	120.4	2.026	2.039	0.994	1
	7	120.5	2.029	2.038	0.996	2
	8	120.3	2.048	2.054	0.997	3
G	1	120.0	2.097	2.190	0.957	0
	2	120.1	2.376	2.383	0.997	1
	3	120.0	2.314	2.240	1.033	2
	4	120.0	2.385	2.410	0.990	3
	5	120.2	2.193	2.343	0.936	0
	6	120.0	2.368	2.403	0.985	1
	7	120.0	2.307	2.319	0.995	2
	8	120.2	2.334	2.358	0.990	3
H	1	49.1	1.944	1.983	0.980	0
	2	49.0	1.972	2.016	0.978	1
	3	49.2	1.920	1.931	0.994	2
	4	48.9	2.004	2.020	0.992	3
	5	48.8	1.925	1.971	0.976	0
	6	48.9	1.787	1.815	0.985	1
	7	49.0	1.915	1.948	0.983	2
	8	48.8	1.954	1.978	0.988	3

* No calibration factors because of excessive non-linearity

Table 2. Results of Tests. (continued)

Gage Type	Gage No.	Resistance R ohms	Calibration increasing strain K_u	Factors decreasing strain K_d	K_u/K_d	No. of Preloads
I	1	120.1	2.133	2.154	0.990	0
	2	120.1	2.143	2.156	0.994	1
	3	120.2	2.143	2.150	0.997	2
	4	120.1	2.144	2.152	0.996	3
	5	120.1	2.138	2.153	0.993	0
	6	120.2	2.145	2.151	0.997	1
	7	120.3	2.152	2.154	0.999	2
	8	120.2	2.152	2.160	0.996	3
J	1	300.3	2.079	2.100	0.990	0
	2	300.3	2.083	2.091	0.996	1
	3	300.8	2.090	2.095	0.998	2
	4	300.2	2.094	2.100	0.997	3
	5	300.4	2.063	2.094	0.985	0
	6	299.9	2.077	2.090	0.994	1
	7	300.1	2.088	2.094	0.997	2
	8	300.0	2.078	2.101	0.989	3
K	1	50.0	2.177	2.210	0.985	0
	2	50.0	2.152	2.161	0.995	1
	3	50.0	2.231	2.239	0.997	2
	4	50.0	2.153	2.165	0.995	3
	5	50.1	2.129	2.147	0.992	0
	6	50.1	2.144	2.154	0.995	1
	7	50.1	2.150	2.158	0.996	2
	8	50.0	2.176	2.177	1.000	3
L	1	119.5	2.283	2.313	0.987	0
	2	119.7	2.180	2.230	0.978	1
	3	120.1	2.183	2.199	0.993	2
	4	119.6	2.225	2.248	0.990	3
	5*	120.5	--	--	--	0
	6**	128.2	--	--	--	1
	7	120.8	2.287	2.296	0.996	2
	8	119.5	2.232	2.238	0.997	3

* No calibration factors because of excessive non-linearity

** Gage observed to have large resistance drift (ascribed to faulty internal solder connection)

Table 2. Results of Tests. (continued)

Gage Type	Gage No.	Resistance R ohms	Calibration increasing strain K_u	Factors decreasing strain K_d	K_u/K_d	No. of Preloads
M	1	120.3	1.982	1.990	0.996	0
	2	120.3	1.974	1.989	0.993	1
	3	120.0	1.975	1.986	0.995	2
	4	120.2	1.981	1.989	0.996	3
	5	120.0	1.965	1.983	0.991	0
	6	120.1	1.978	1.986	0.996	1
	7	120.4	1.959	1.970	0.994	2
	8	120.0	1.986	1.991	0.997	3
N	1	504.0	3.490	3.492	1.000	0
	2	503.7	3.469	3.486	0.995	1
	3	504.7	3.488	3.475	1.004	2
	4	504.9	3.490	3.490	1.000	3
	5	503.6	3.451	3.466	0.996	0
	6	505.2	3.471	3.483	0.996	1
	7	504.6	3.492	3.473	1.005	2
	8	503.5	3.489	3.474	1.004	3
O	1	100.3	2.042	2.078	0.983	0
	2	100.0	2.065	2.071	0.997	1
	3	100.3	2.061	2.073	0.994	2
	4	99.9	2.103	2.094	1.004	3
	5	100.0	2.071	2.108	0.982	0
	6	100.0	2.110	2.113	0.998	1
	7	100.3	2.092	2.108	0.993	2
	8	99.9	2.089	2.098	0.996	3

Table 3. Sequence of Gages in Order of Increasing Strain Deviations from an Average Straight Line

Gage Type	Total range of strain deviations*
	10^6
I	28
B	32
M	34
N	38
J	41
F	43
D	49
C	56
A	58
O	63
K	99
E	176
H	>173
G	>249
L	>276

* Width of a vertical band enclosing all points in each of figures 9 to 23.

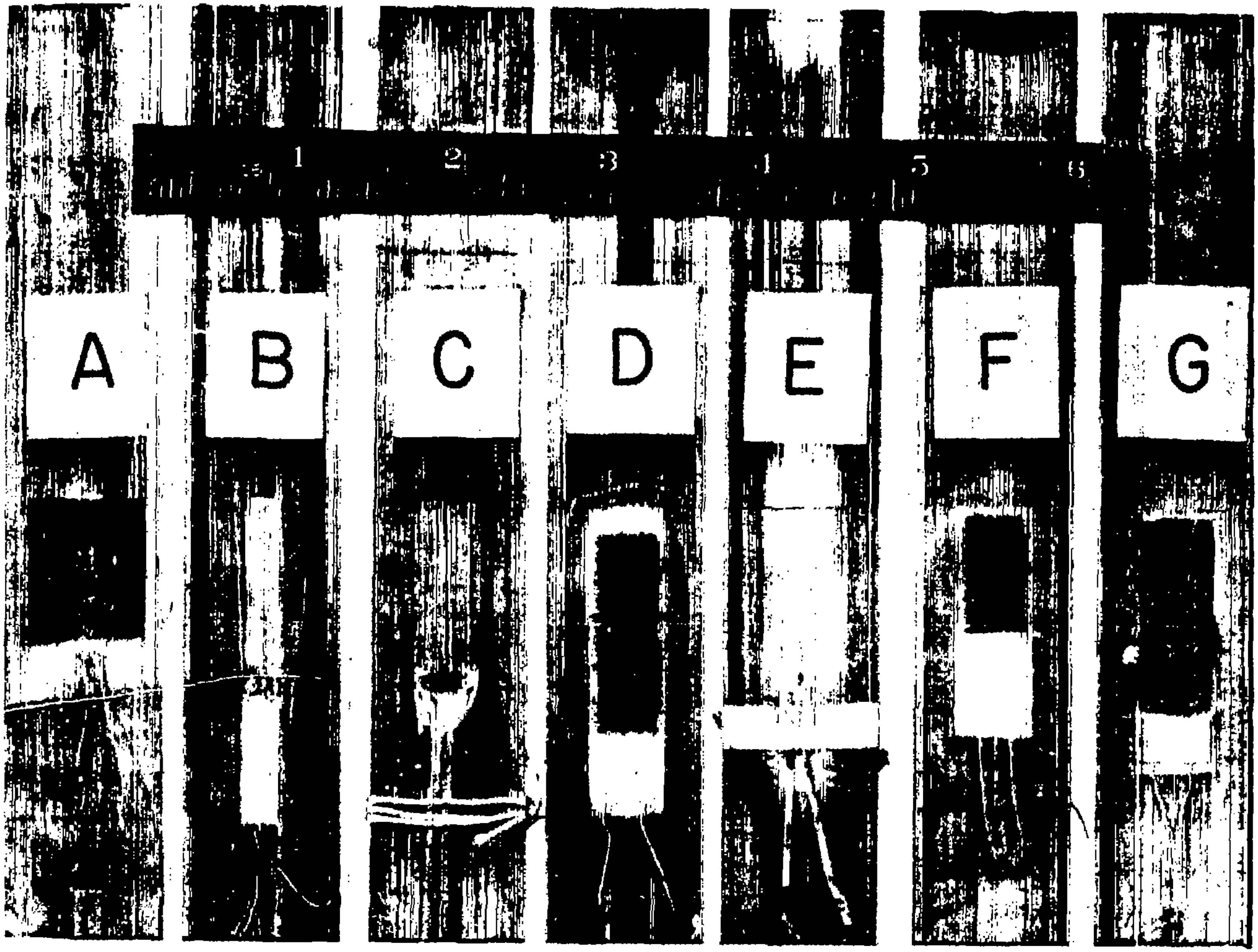

Figure 1.- Test gages of types A to G attached to calibration strips.

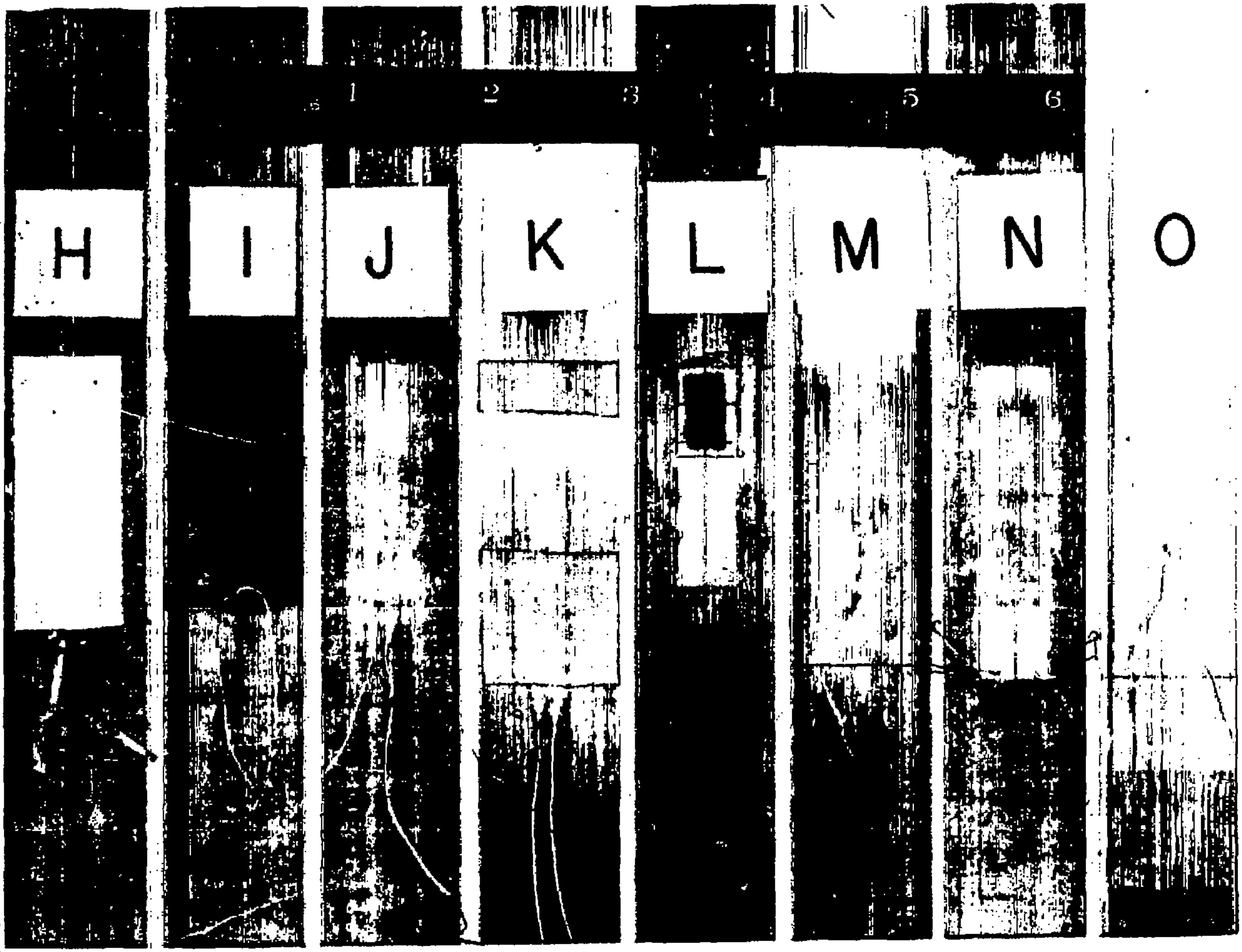

Figure 2.-- Test gages of types H to O attached to calibration strips.

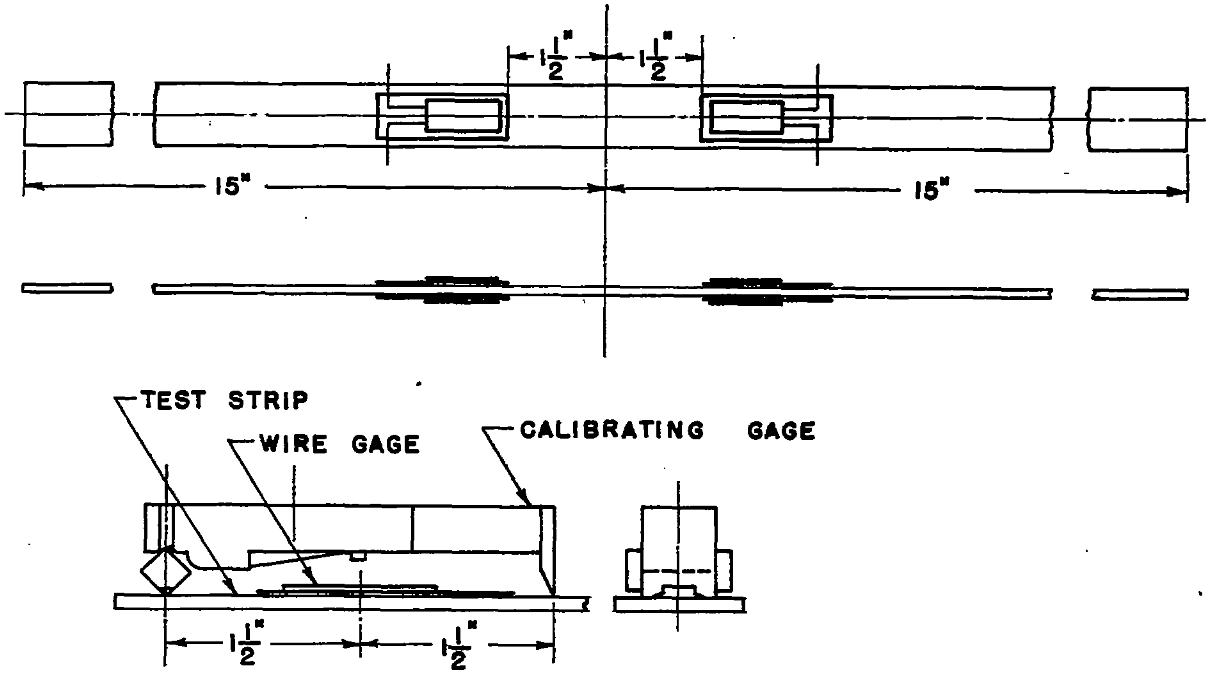

Figure 3.- Location of wire strain gages on calibration strip and position of Tuckerman gage during calibration.

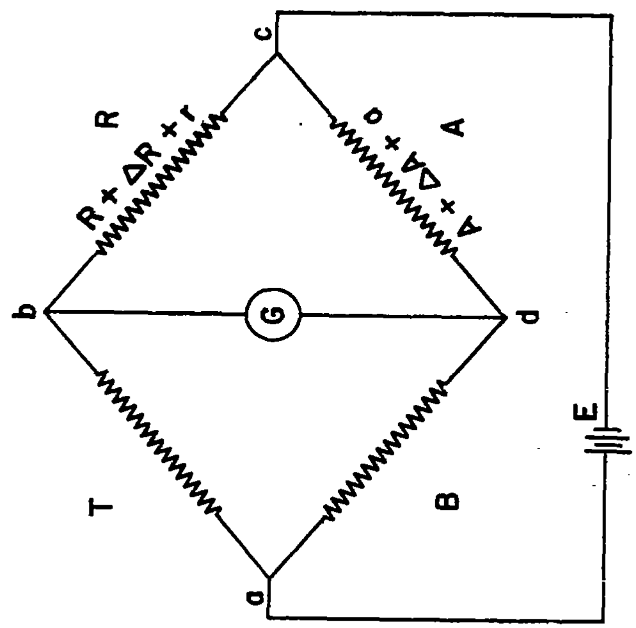

Figure 4.- Wheatstone bridge for resistance measurements. R and T denote the test and compensating wire strain gages respectively. A and B represent the two arms of the ratio set.

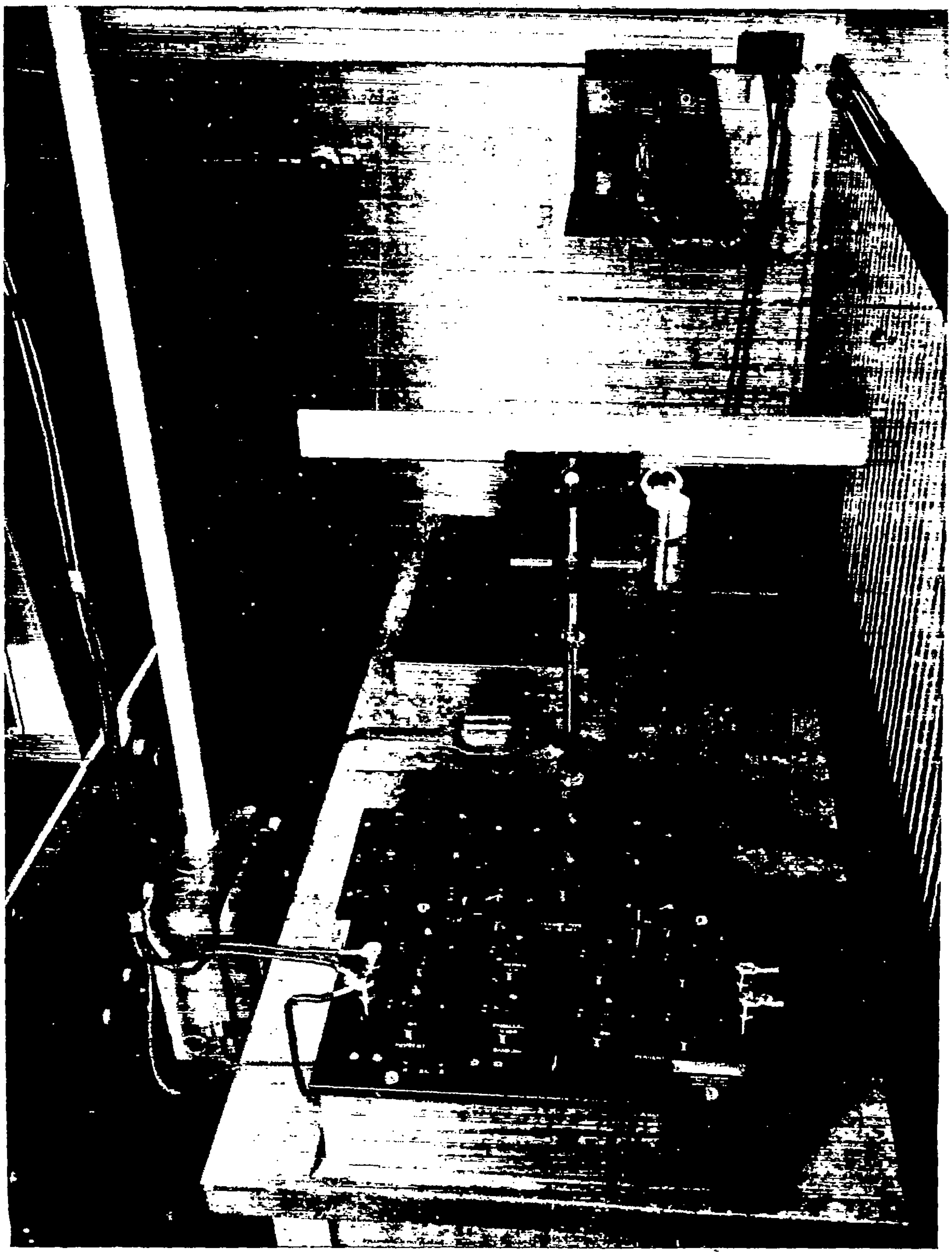

Figure 6.- Laboratory set up for resistance measurements.

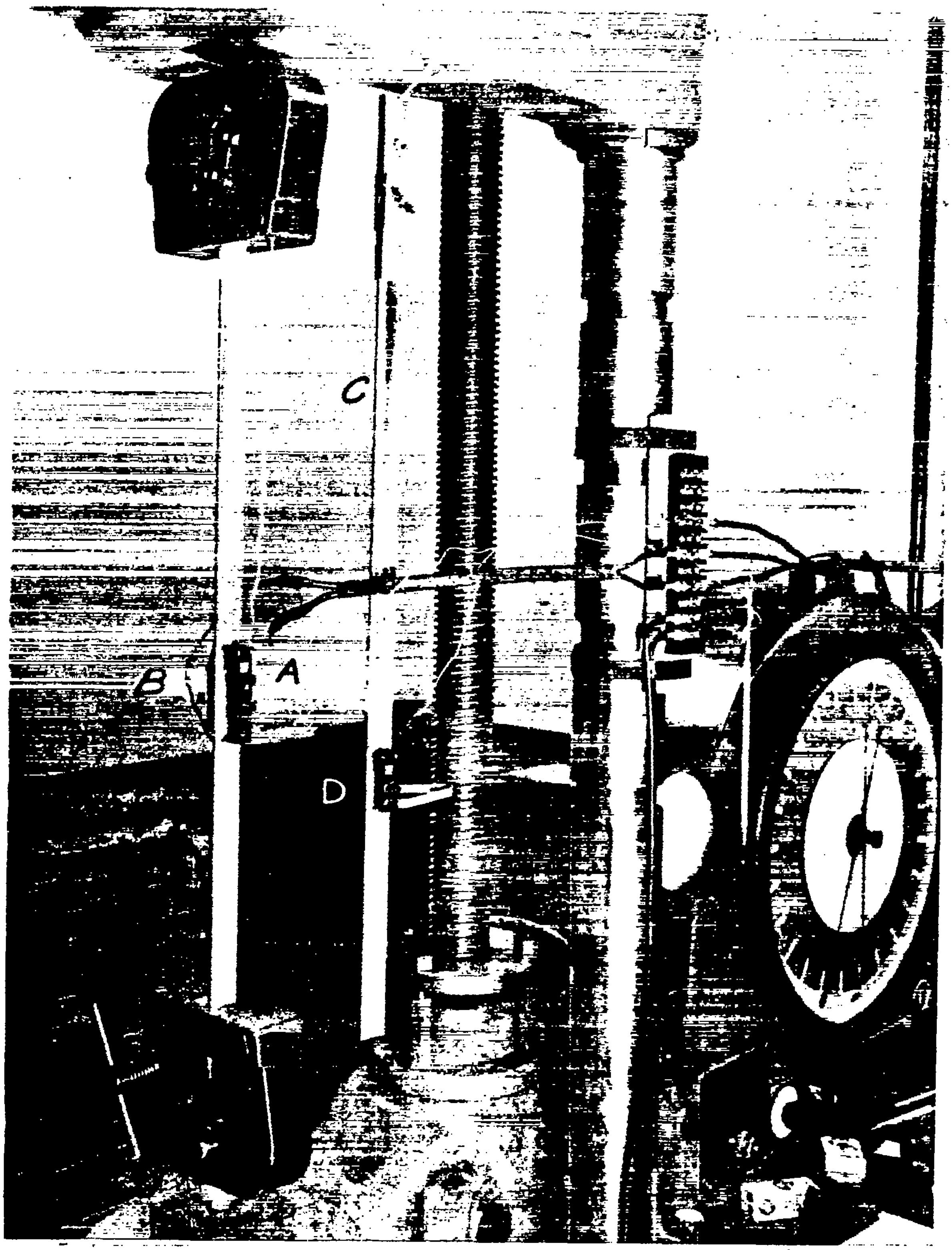

Figure 7.- Laboratory set up for strain measurements.

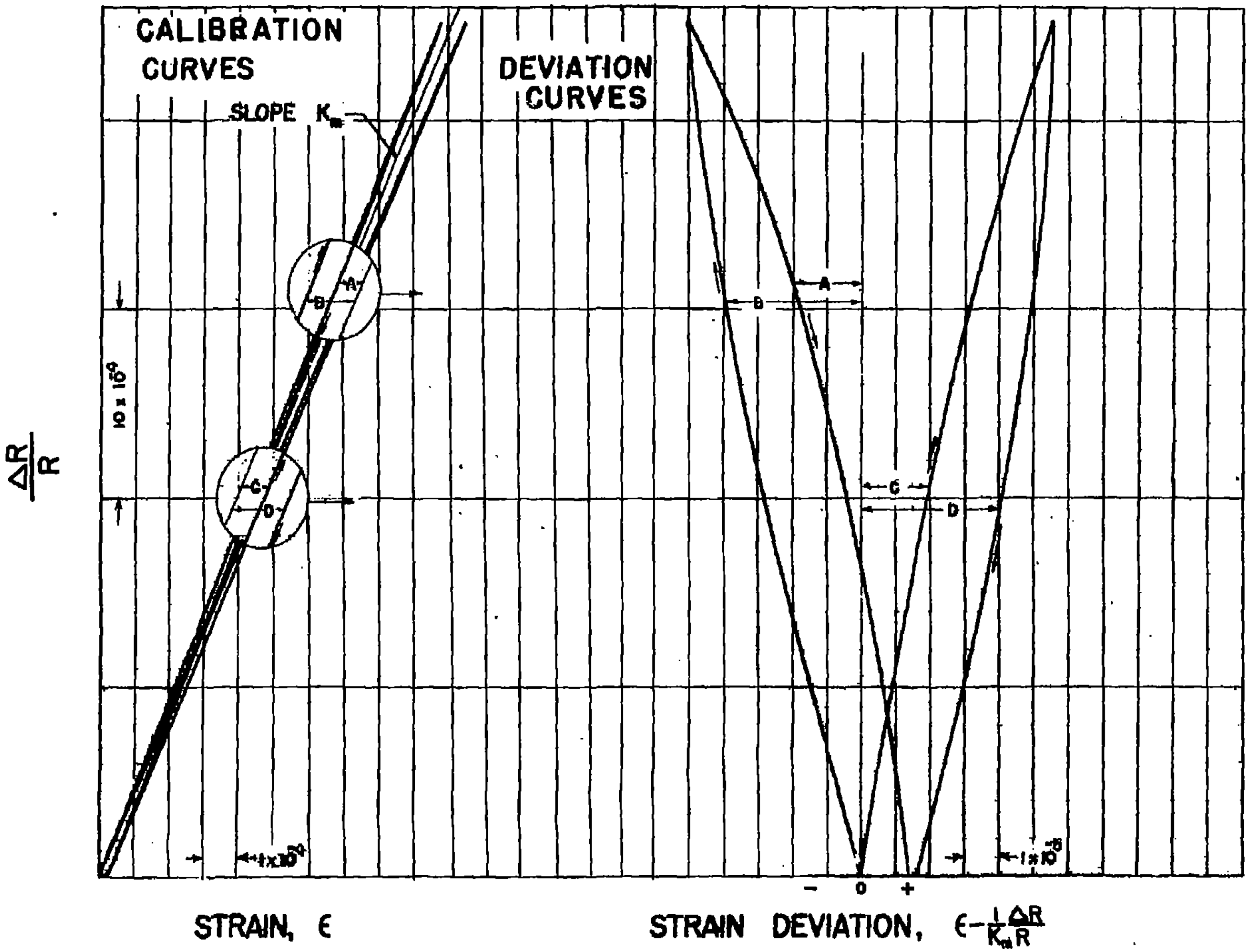

Figure 8.- Hypothetical calibration and strain deviation curves showing the relation between them.

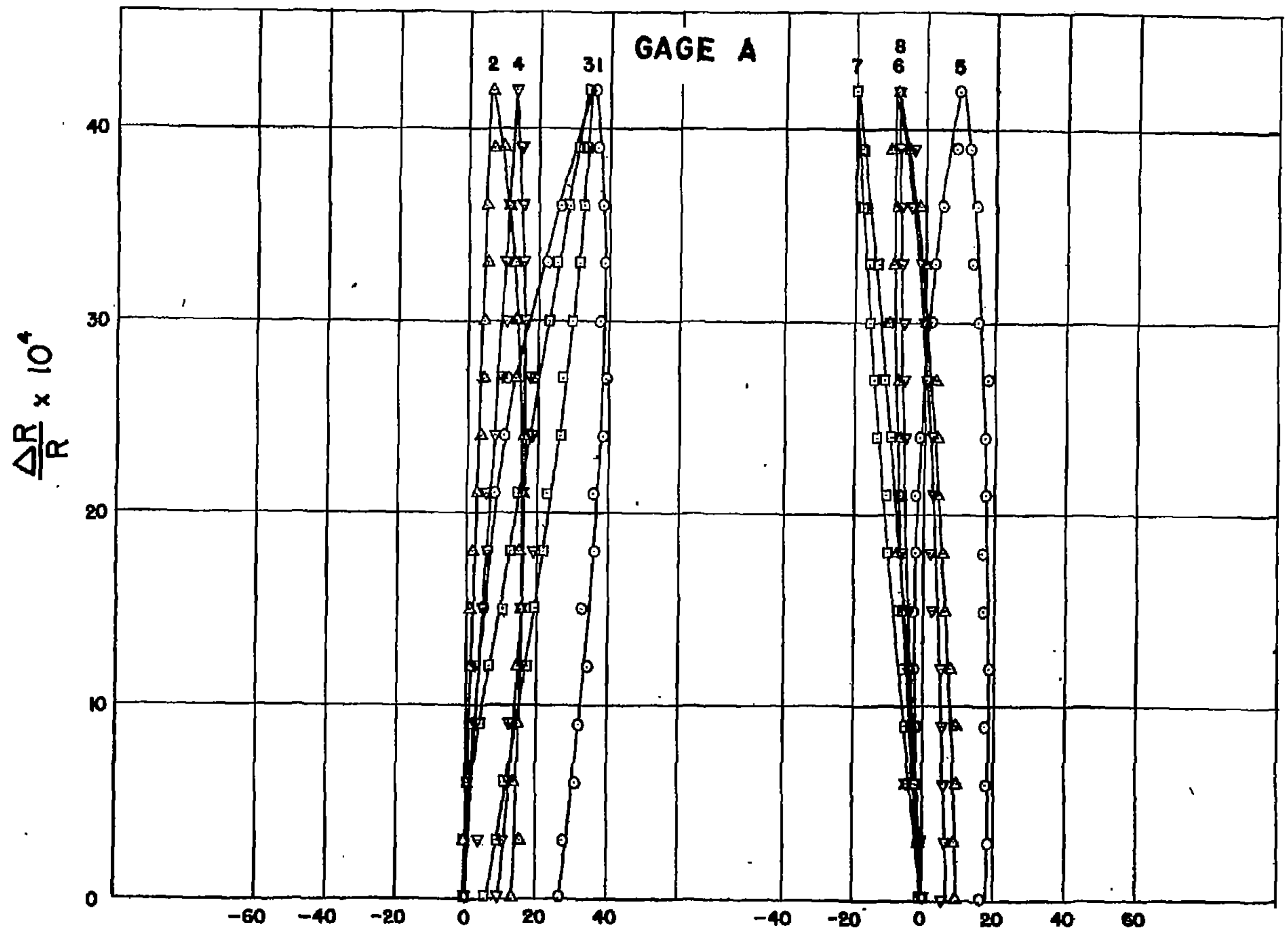
GAGE A
2
4
31
7
8
6
5
40
30
20
10
0
-60
-40
-20
0
20
40
-40
-20
0
20
40
60
$\frac{\Delta R}{R} \times 10^4$
STRAIN DEVIATION, PARTS PER MILLION, $\left[\epsilon - \frac{1}{K_m}\frac{\Delta R}{R}\right] 10^6$

FIG. 9

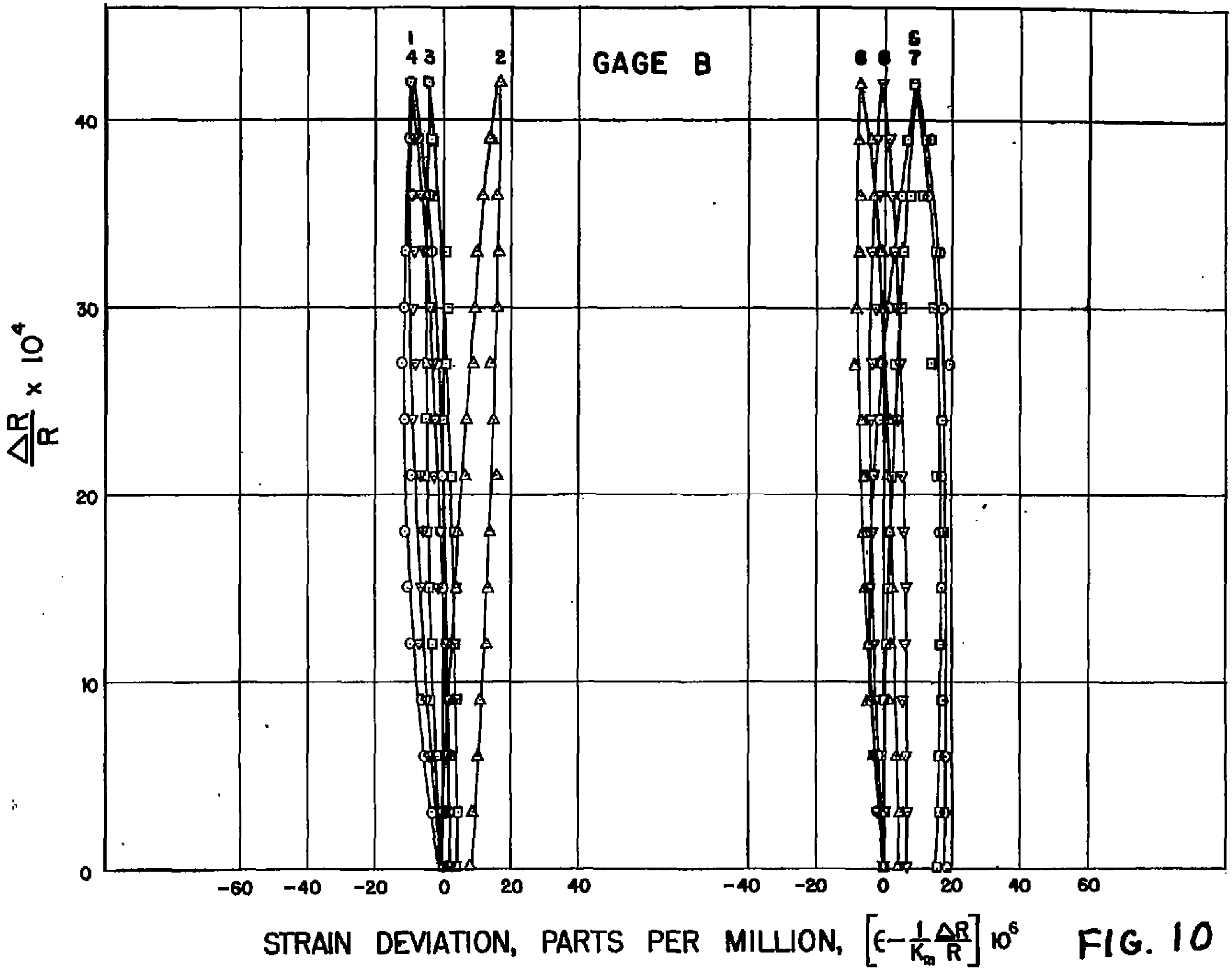
GAGE B
1
4 3
2
5
6 8 7
0
10
20
30
40
$\frac{\Delta R}{R} \times 10^4$
-60 -40 -20 0 20 40
-40 -20 0 20 40 60
STRAIN DEVIATION, PARTS PER MILLION, $\left[\epsilon - \frac{1}{K_m}\frac{\Delta R}{R}\right] 10^6$

FIG. 10

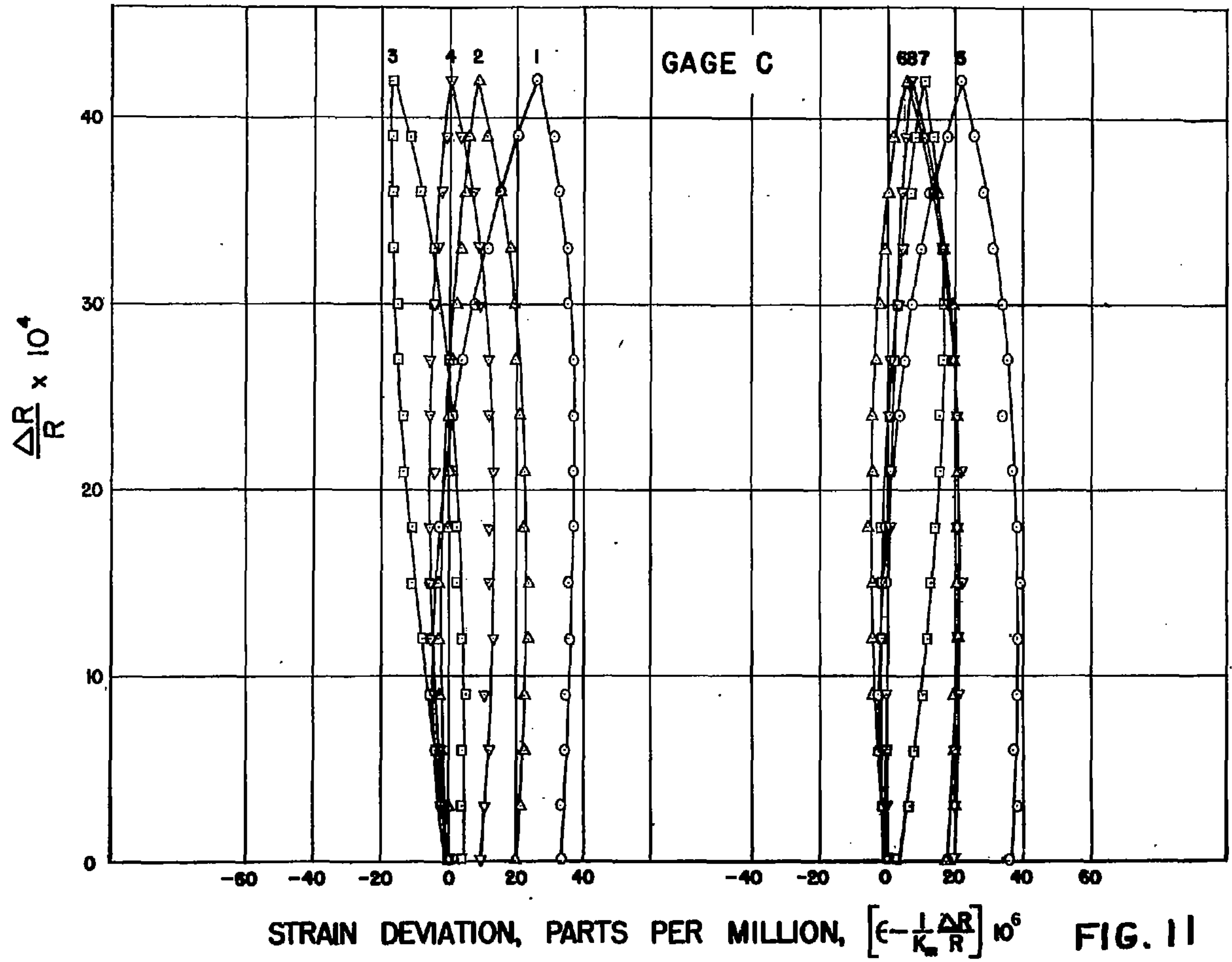
GAGE C
3
4
2
1
687
5
$\frac{\Delta R}{R} \times 10^4$
0
10
20
30
40
-60
-40
-20
0
20
40
-40
-20
0
20
40
60
STRAIN DEVIATION, PARTS PER MILLION, $\left[\epsilon - \frac{1}{K_m}\frac{\Delta R}{R}\right]10^6$

FIG. 11

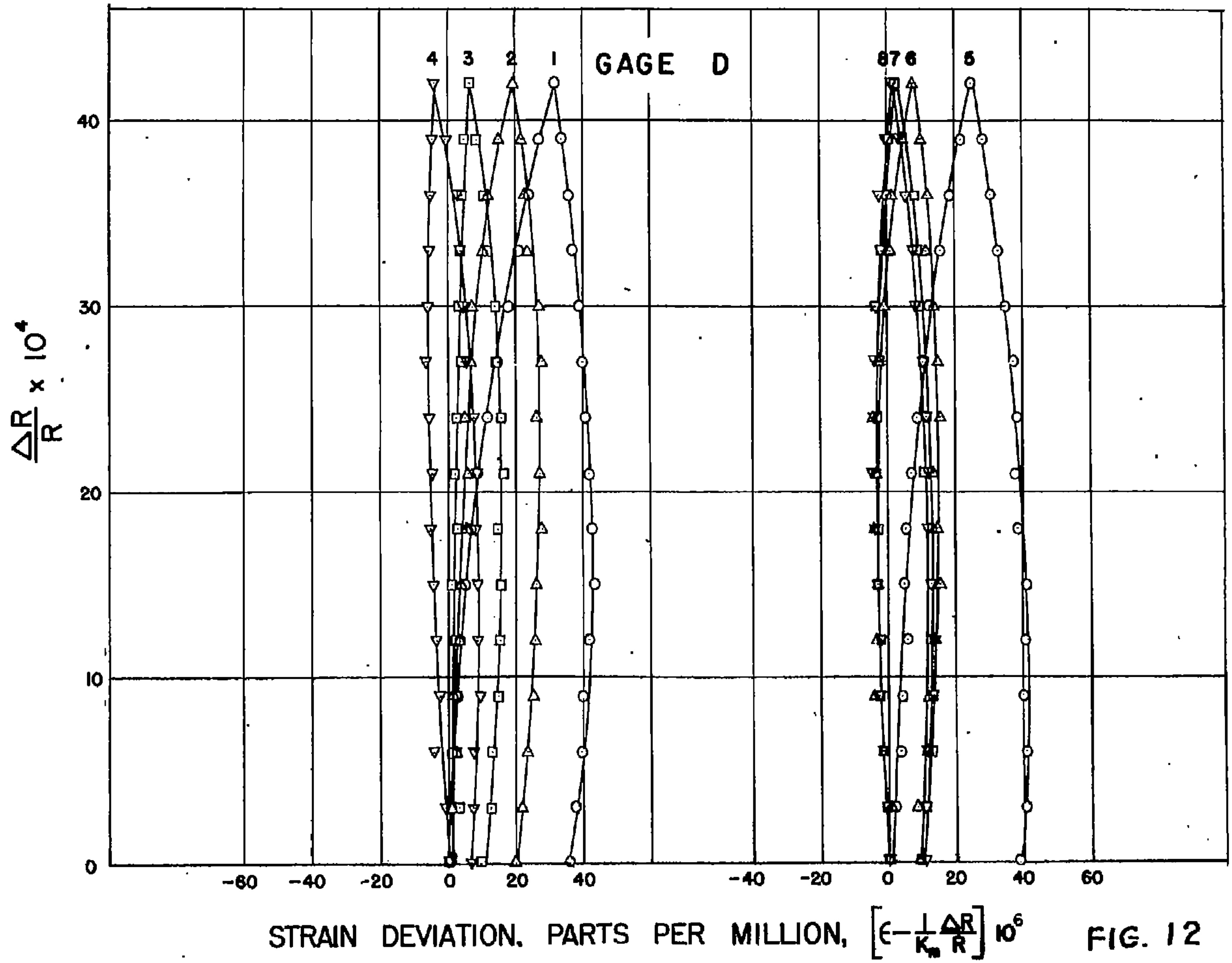
GAGE D
4 3 2 1
8 7 6 5
$\frac{\Delta R}{R} \times 10^4$
0
10
20
30
40
-60 -40 -20 0 20 40
-40 -20 0 20 40 60
STRAIN DEVIATION, PARTS PER MILLION, $\left[\epsilon - \frac{1}{K_m}\frac{\Delta R}{R}\right] 10^6$

FIG. 12

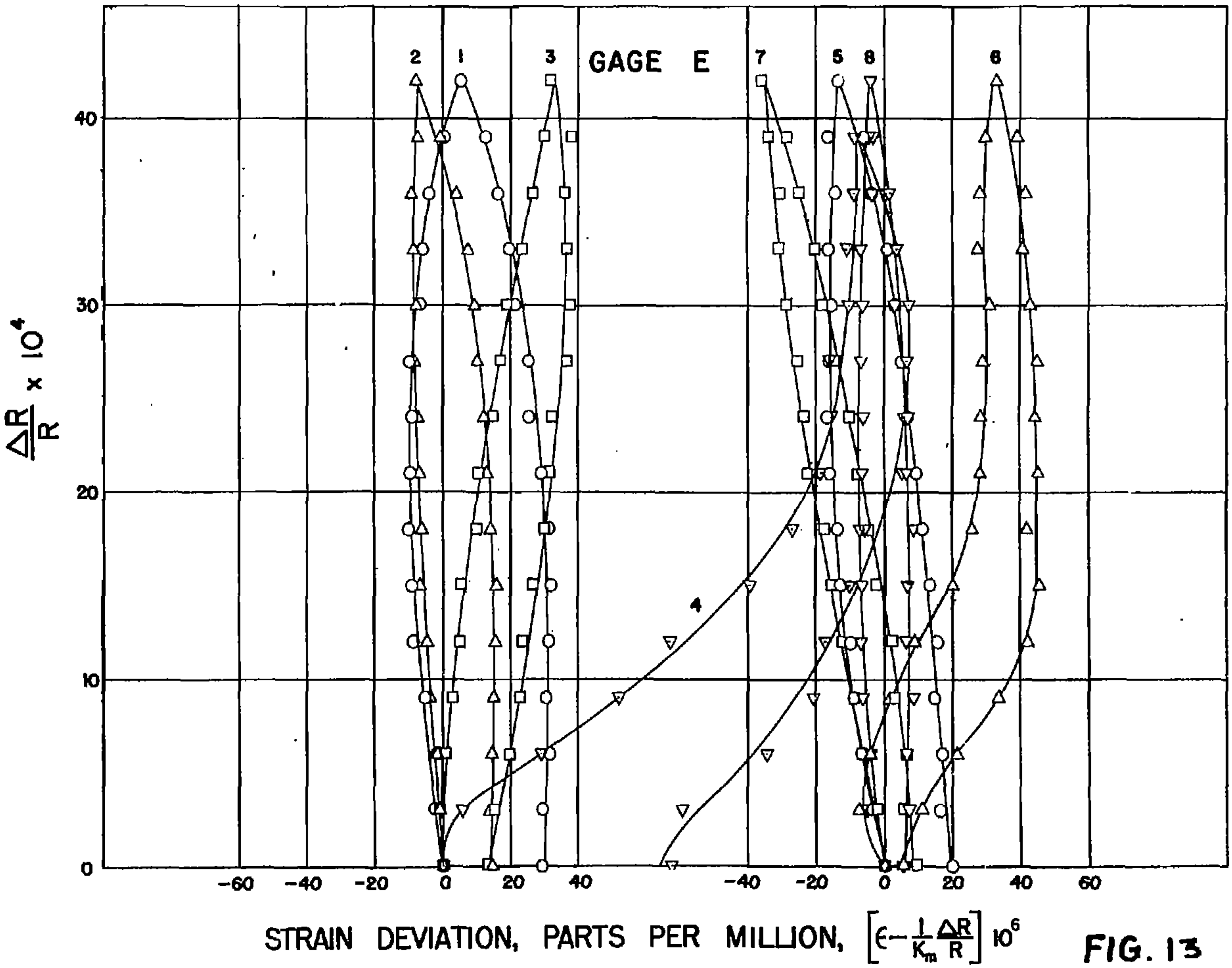
GAGE E
2
1
3
7
5
8
6
4
$\frac{\Delta R}{R} \times 10^4$
0
10
20
30
40
-60
-40
-20
0
20
40
-40
-20
0
20
40
60
STRAIN DEVIATION, PARTS PER MILLION, $\left[\epsilon - \frac{1}{K_m}\frac{\Delta R}{R}\right] 10^6$

FIG. 13

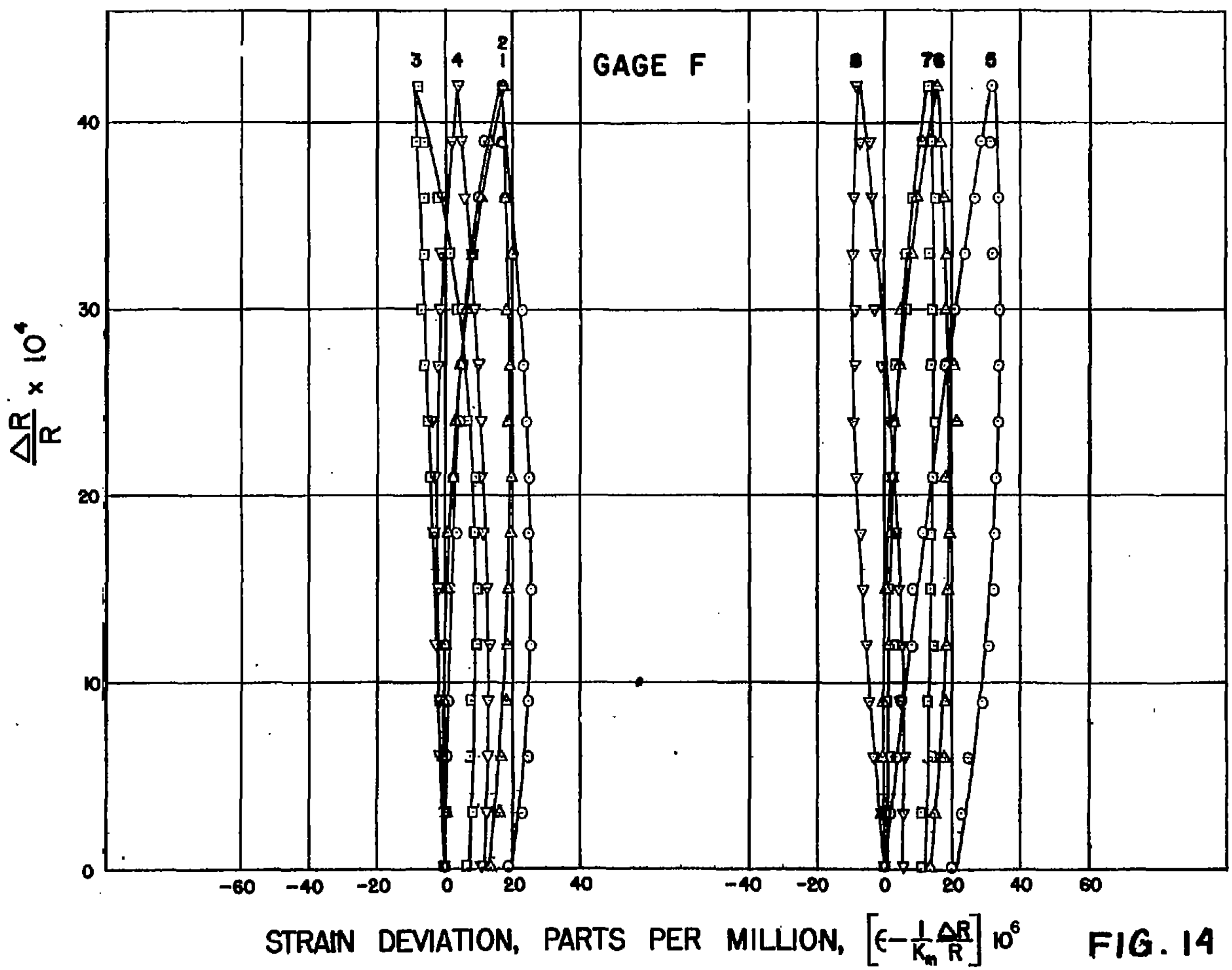
GAGE F
3
4
2
1
8
7
6
5
0
10
20
30
40
$\frac{\Delta R}{R} \times 10^4$
-60
-40
-20
0
20
40
-40
-20
0
20
40
60
STRAIN DEVIATION, PARTS PER MILLION, $\left[\epsilon - \frac{1}{K_m}\frac{\Delta R}{R}\right] 10^6$

FIG. 14

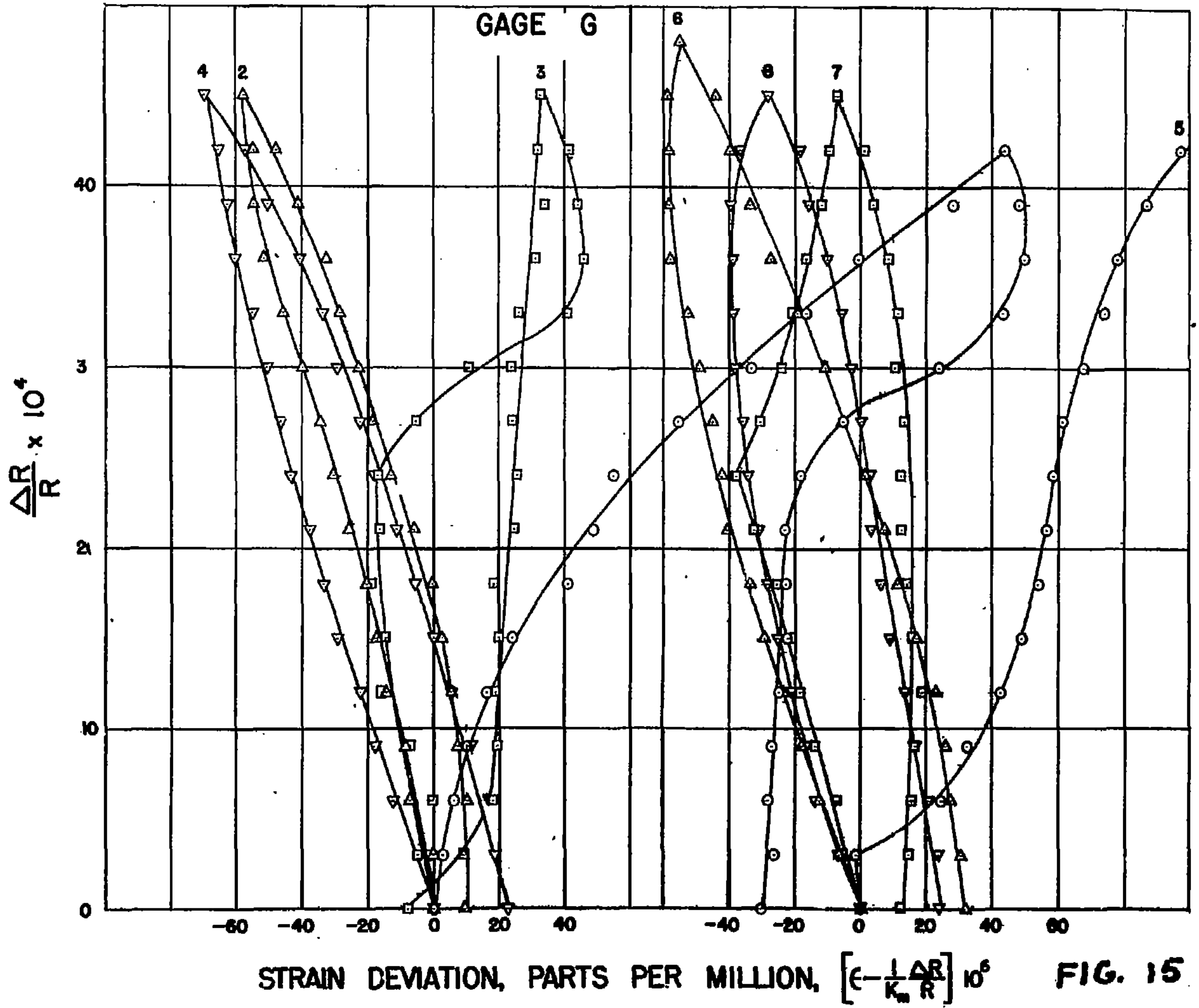
GAGE G
4
2
3
6
8
7
5
$\frac{\Delta R}{R} \times 10^4$
STRAIN DEVIATION, PARTS PER MILLION, $\left[\epsilon - \frac{1}{K_m}\frac{\Delta R}{R}\right] 10^6$

FIG. 15

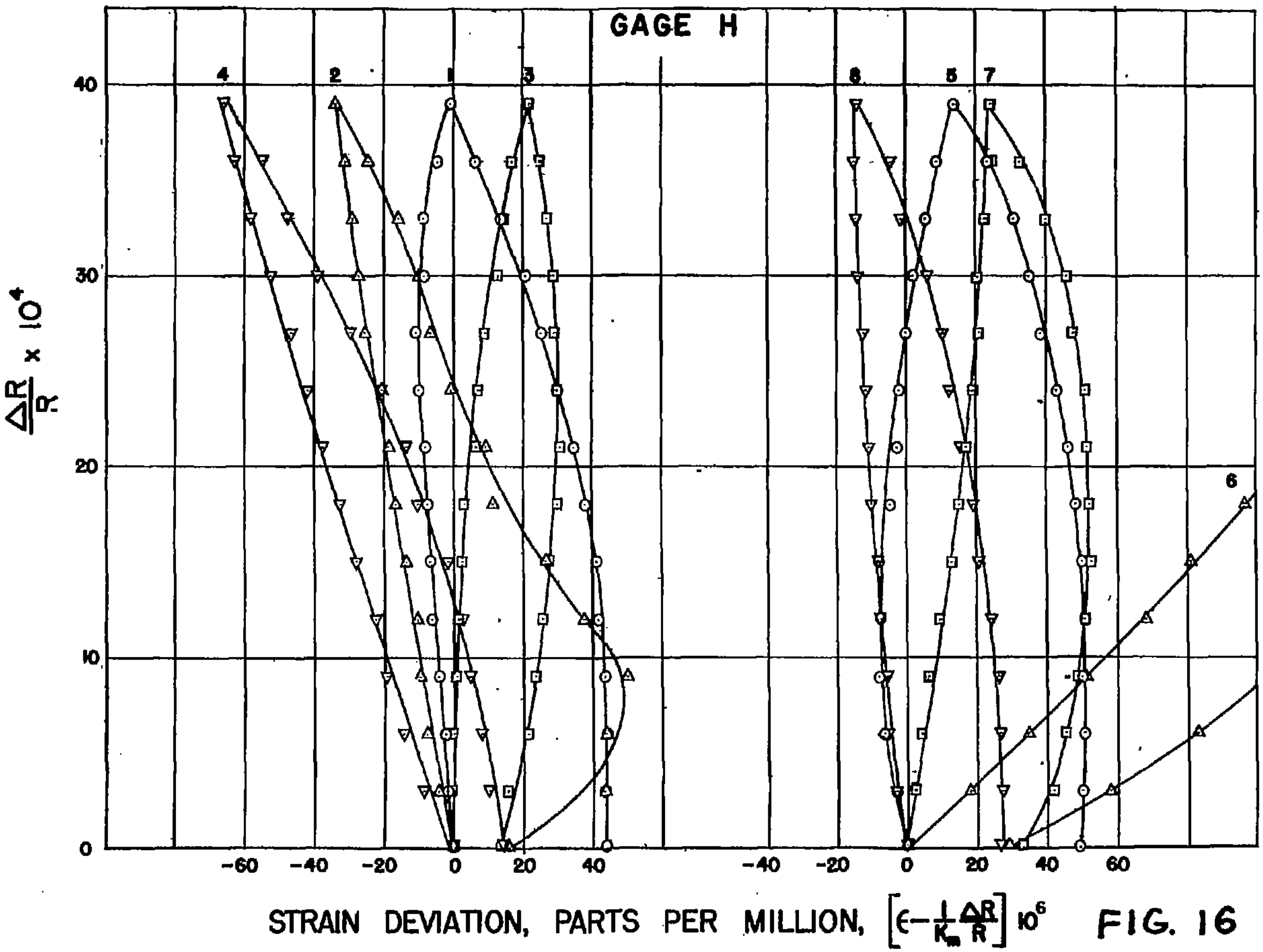
GAGE H
4
2
1
3
8
5
7
6
40
30
20
10
0
-60
-40
-20
0
20
40
-40
-20
0
20
40
60
$\frac{\Delta R}{R} \times 10^4$
STRAIN DEVIATION, PARTS PER MILLION, $\left[\epsilon - \frac{1}{K_m}\frac{\Delta R}{R}\right] 10^6$

FIG. 16

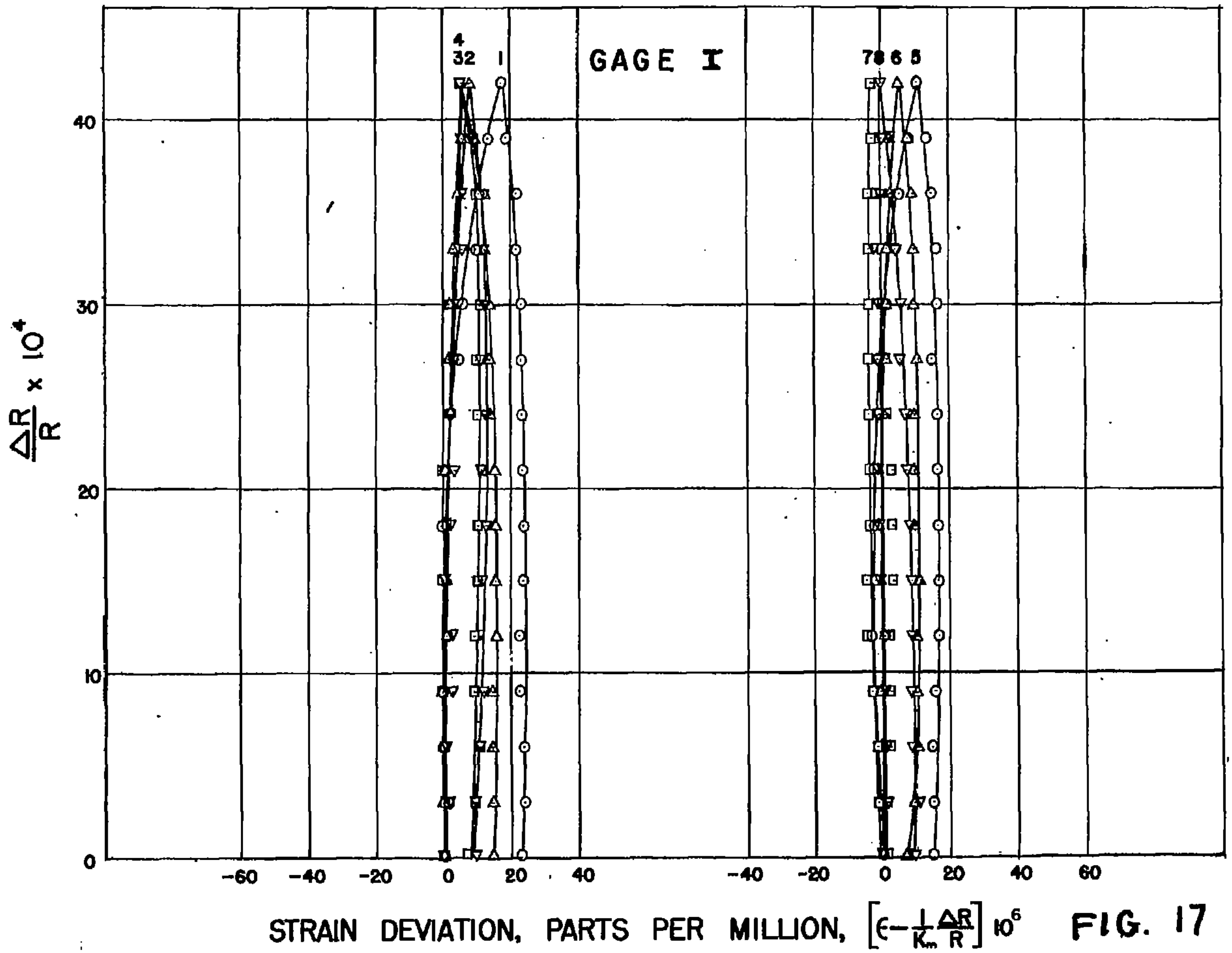
GAGE I
4
32
1
78
6
5
$\frac{\Delta R}{R} \times 10^4$
0
10
20
30
40
-60
-40
-20
0
20
40
-40
-20
0
20
40
60
STRAIN DEVIATION, PARTS PER MILLION, $\left[\epsilon - \frac{1}{K_m}\frac{\Delta R}{R}\right] 10^6$

FIG. 17

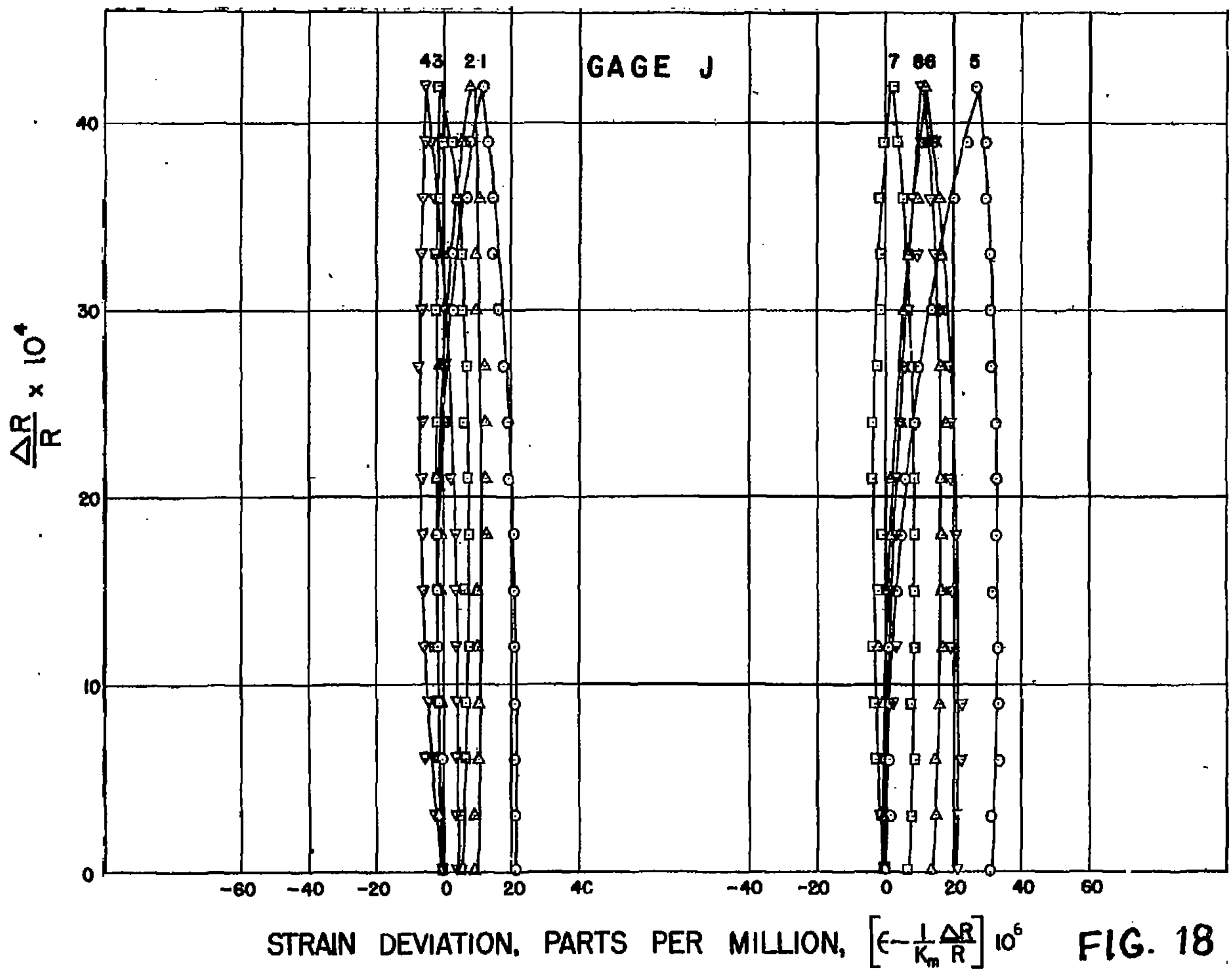
GAGE J
43
2 1
7
8 6
5
$\frac{\Delta R}{R} \times 10^4$
0
10
20
30
40
-60
-40
-20
0
20
40
-40
-20
0
20
40
60
STRAIN DEVIATION, PARTS PER MILLION, $\left[\epsilon - \frac{1}{K_m}\frac{\Delta R}{R}\right] 10^6$

FIG. 18

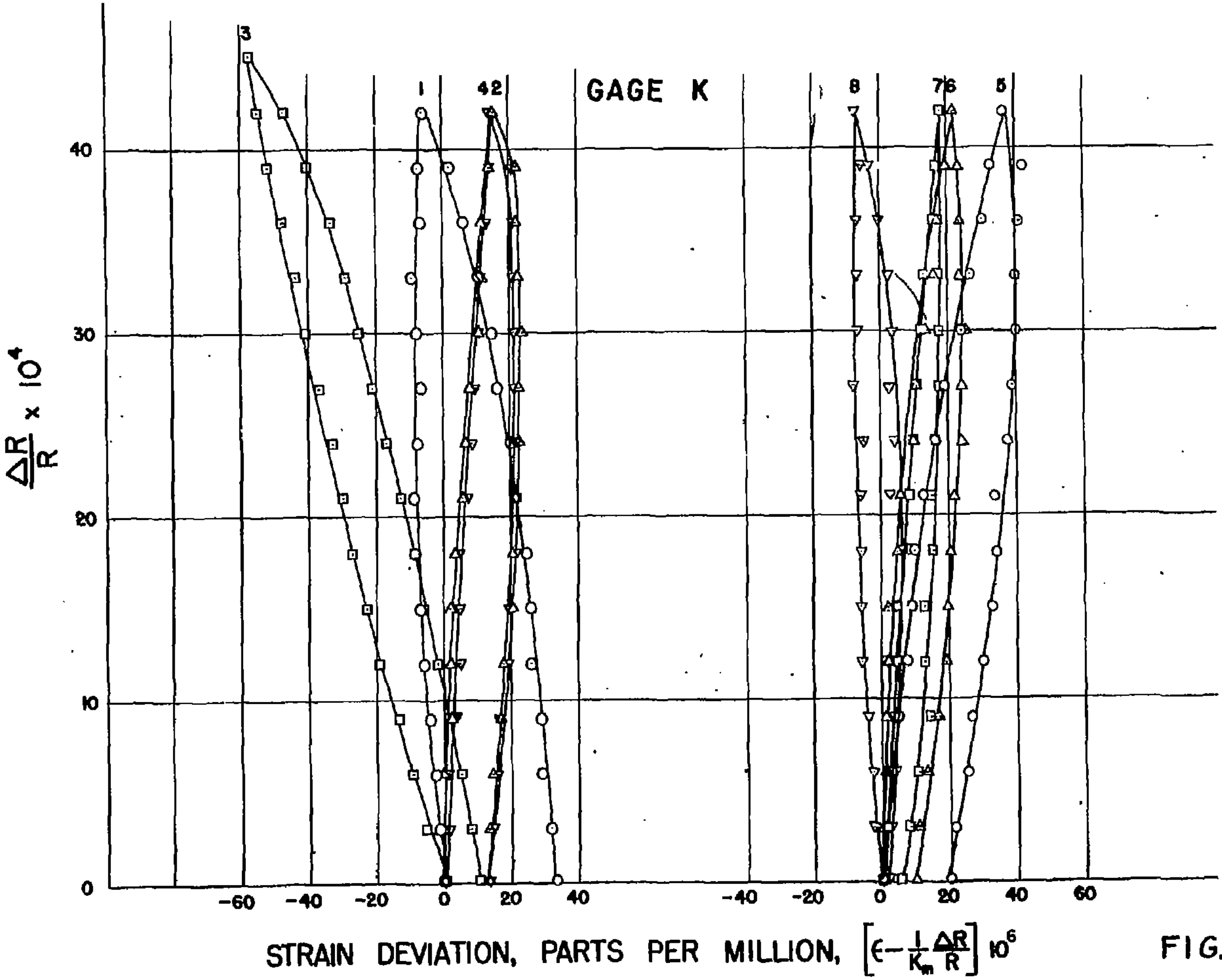
GAGE K
3
1
42
8
76
5
40
30
20
10
0
-60
-40
-20
0
20
40
-40
-20
0
20
40
60
$\frac{\Delta R}{R} \times 10^4$
STRAIN DEVIATION, PARTS PER MILLION, $\left[\epsilon - \frac{1}{K_m}\frac{\Delta R}{R}\right] 10^6$

FIG. 19

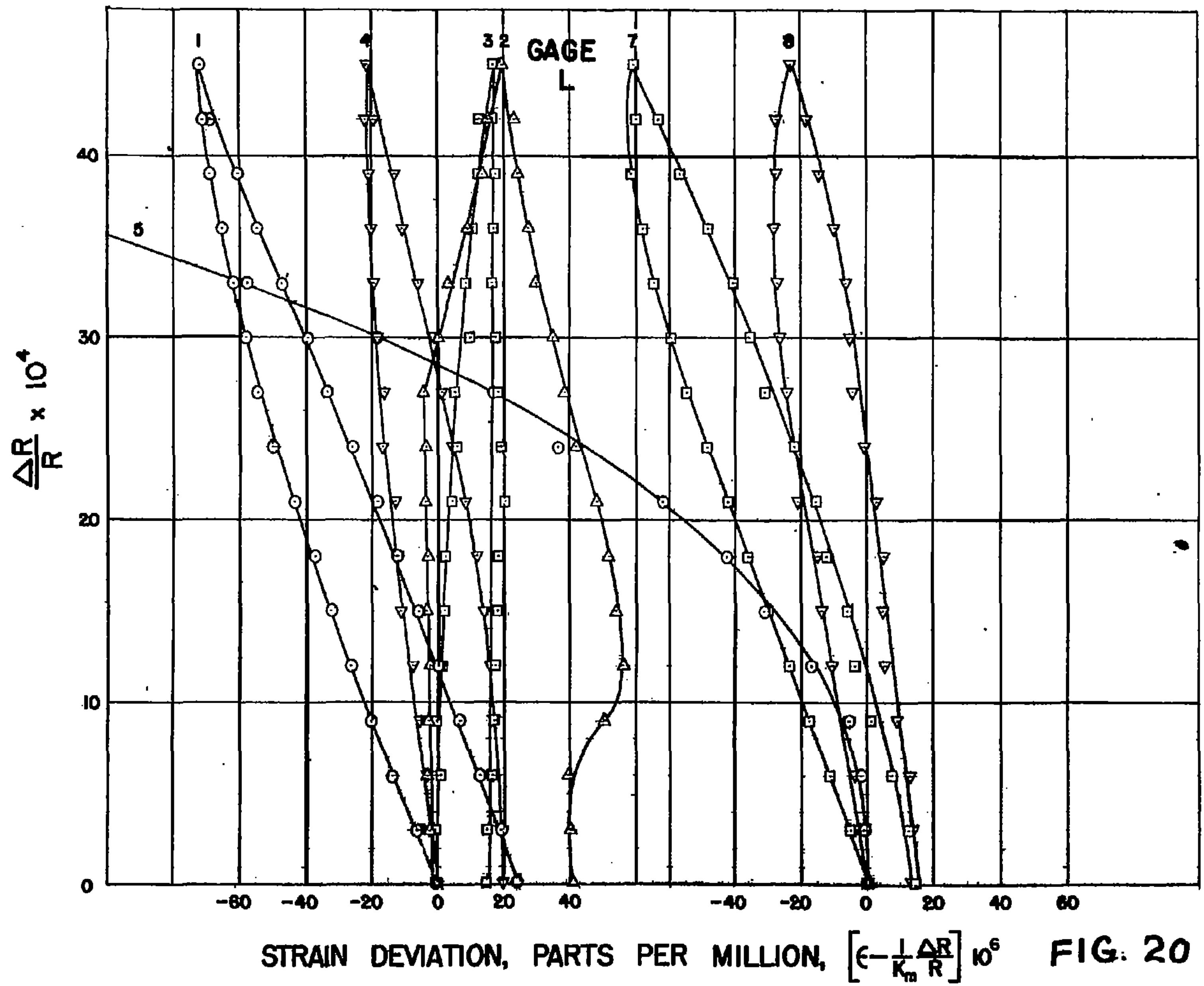
GAGE
L
1
4
3
2
7
8
5
0
10
20
30
40
-60
-40
-20
0
20
40
-40
-20
0
20
40
60
$\frac{\Delta R}{R} \times 10^4$
STRAIN DEVIATION, PARTS PER MILLION, $\left[\epsilon - \frac{1}{K_m}\frac{\Delta R}{R}\right] 10^6$

FIG. 20

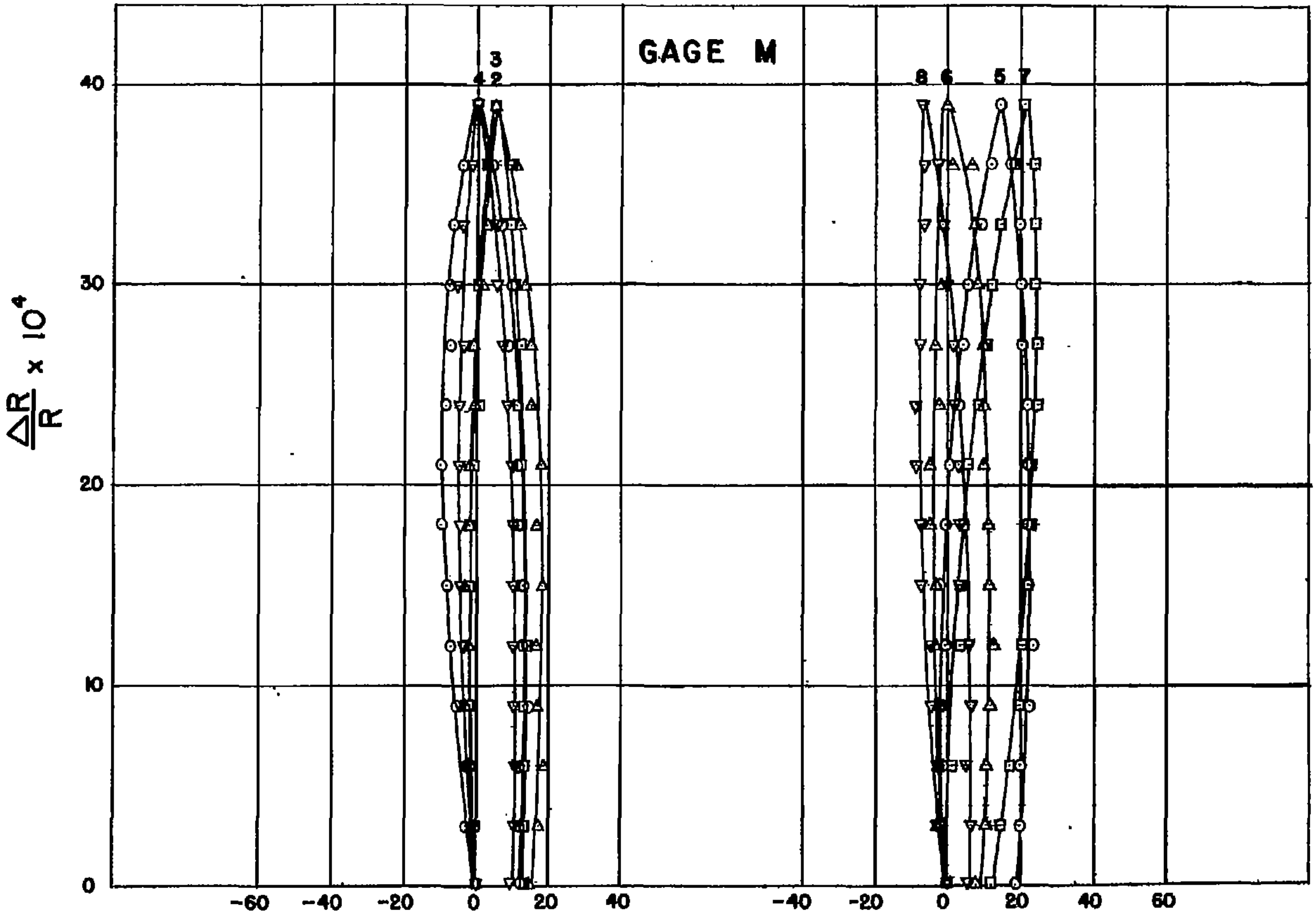
GAGE M
4 3 2
8 6 5 7
$\frac{\Delta R}{R} \times 10^4$
0
10
20
30
40
-60 -40 -20 0 20 40
-40 -20 0 20 40 60
STRAIN DEVIATION, PARTS PER MILLION, $\left[\epsilon - \frac{1}{K_m}\frac{\Delta R}{R}\right] 10^6$

FIG. 21

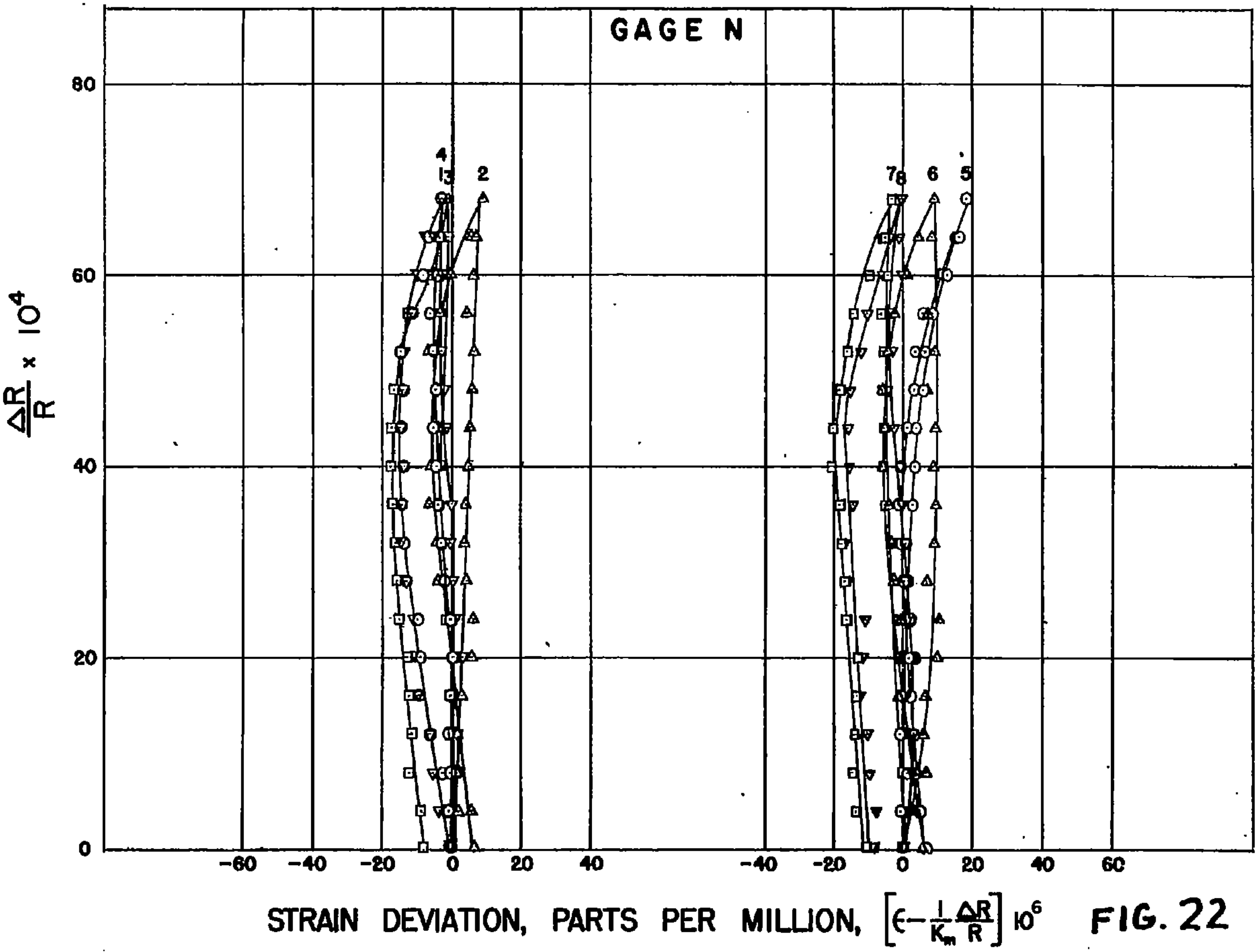
GAGE N
4
1 3
2
7 8
6
5
80
60
40
20
0
-60
-40
-20
0
20
40
-40
-20
0
20
40
60
$\frac{\Delta R}{R} \times 10^4$
STRAIN DEVIATION, PARTS PER MILLION, $\left[\epsilon - \frac{1}{K_m}\frac{\Delta R}{R}\right] 10^6$

FIG. 22

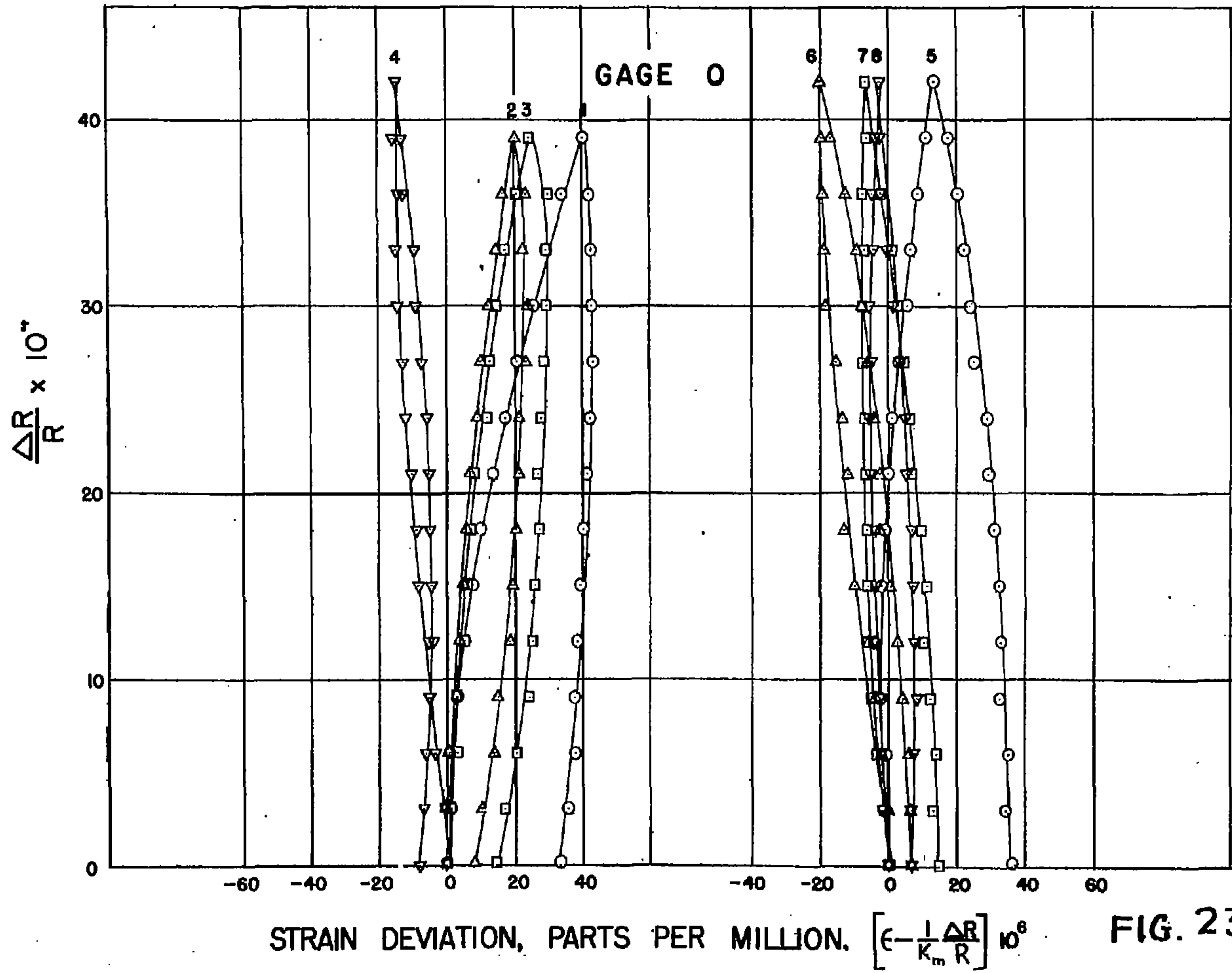
GAGE O
4
2 3
1
6
7 8
5
$\frac{\Delta R}{R} \times 10^4$
0
10
20
30
40
-60
-40
-20
0
20
40
-40
-20
0
20
40
60
STRAIN DEVIATION, PARTS PER MILLION, $\left[\epsilon - \frac{1}{K_m}\frac{\Delta R}{R}\right] 10^6$

FIG. 23

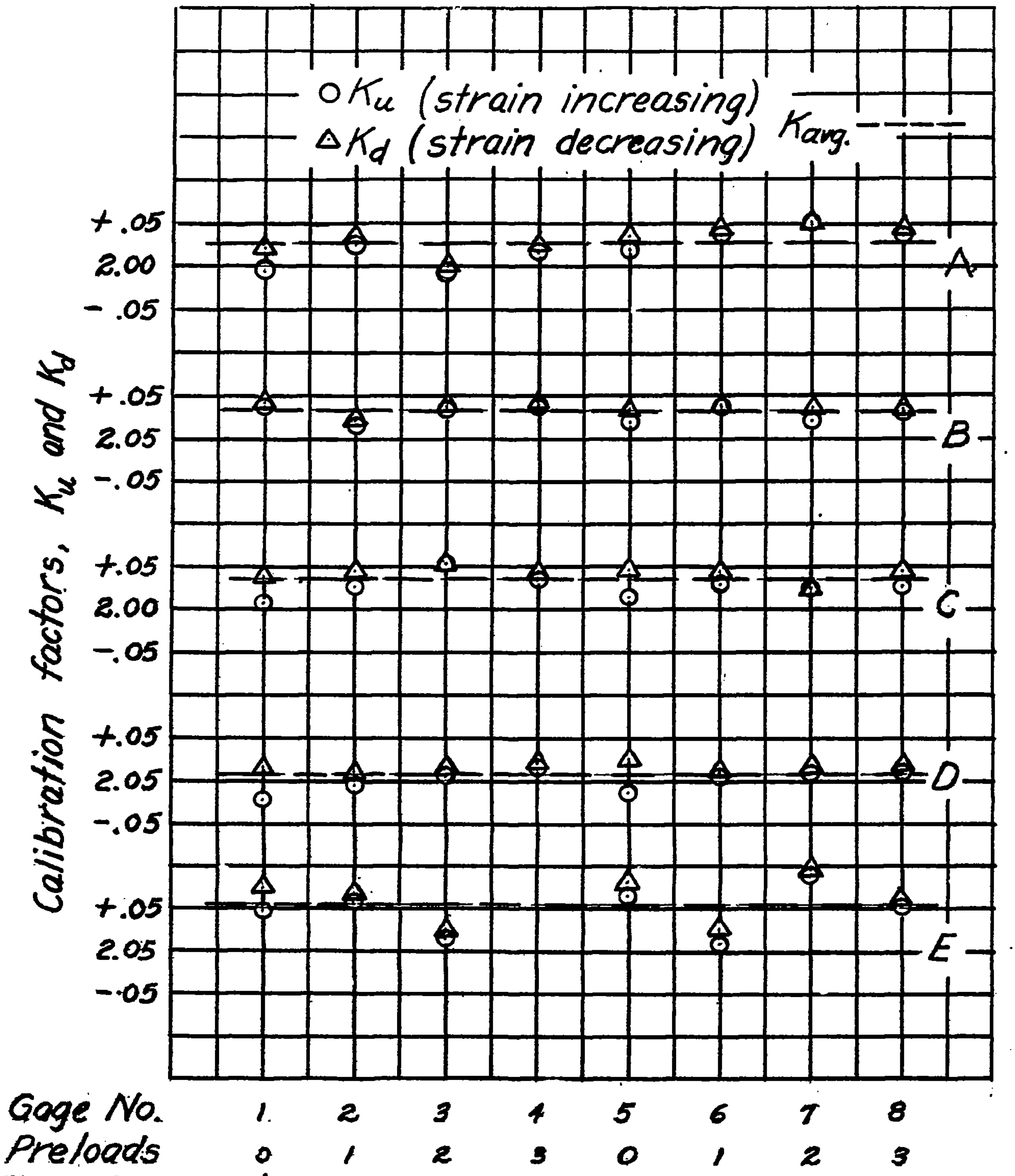

Figure 24.- Calibration factors vs. gage number and preloads (from table 1).

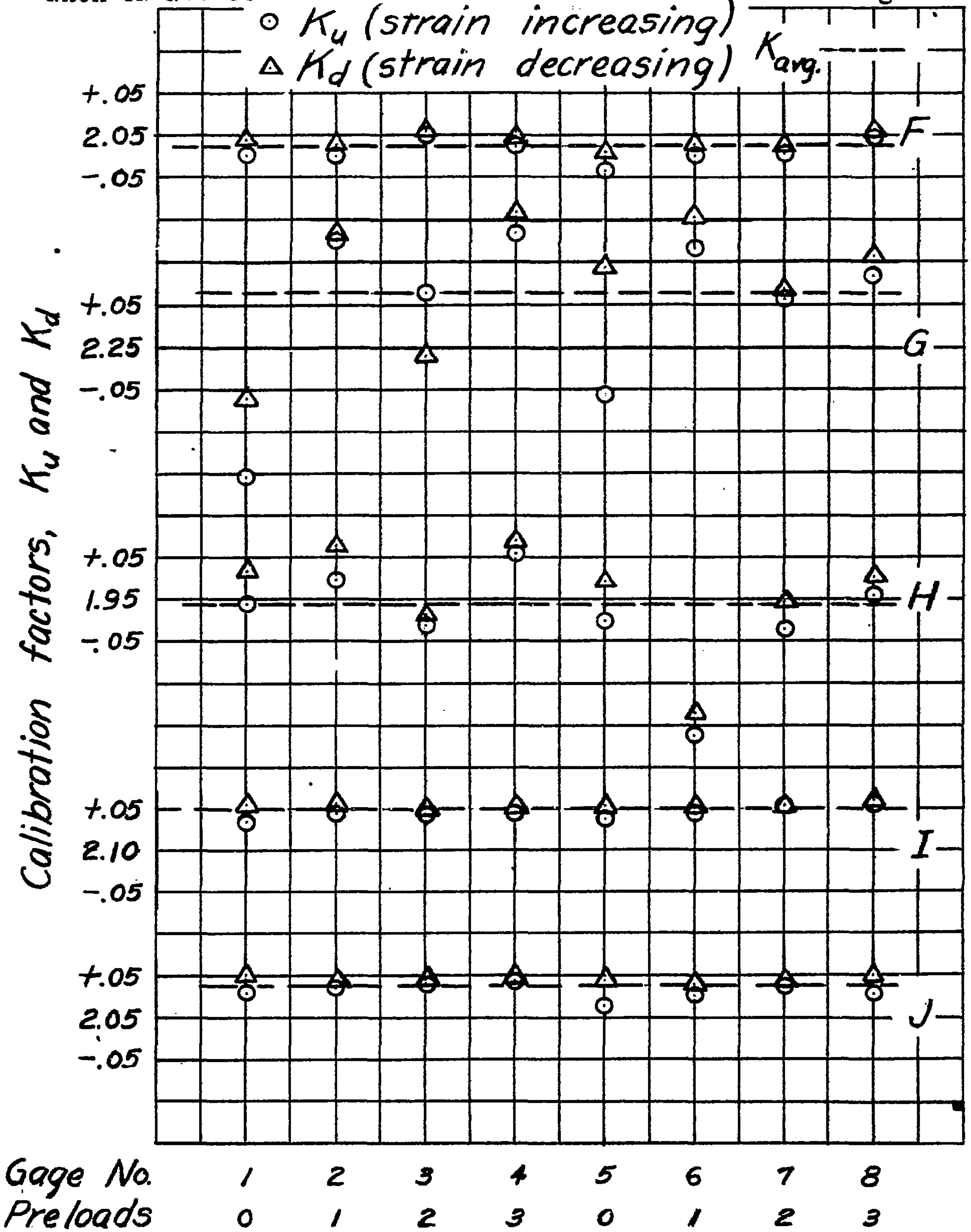

Figure 25.- Calibration factors vs gage number and preloads (from table 1).

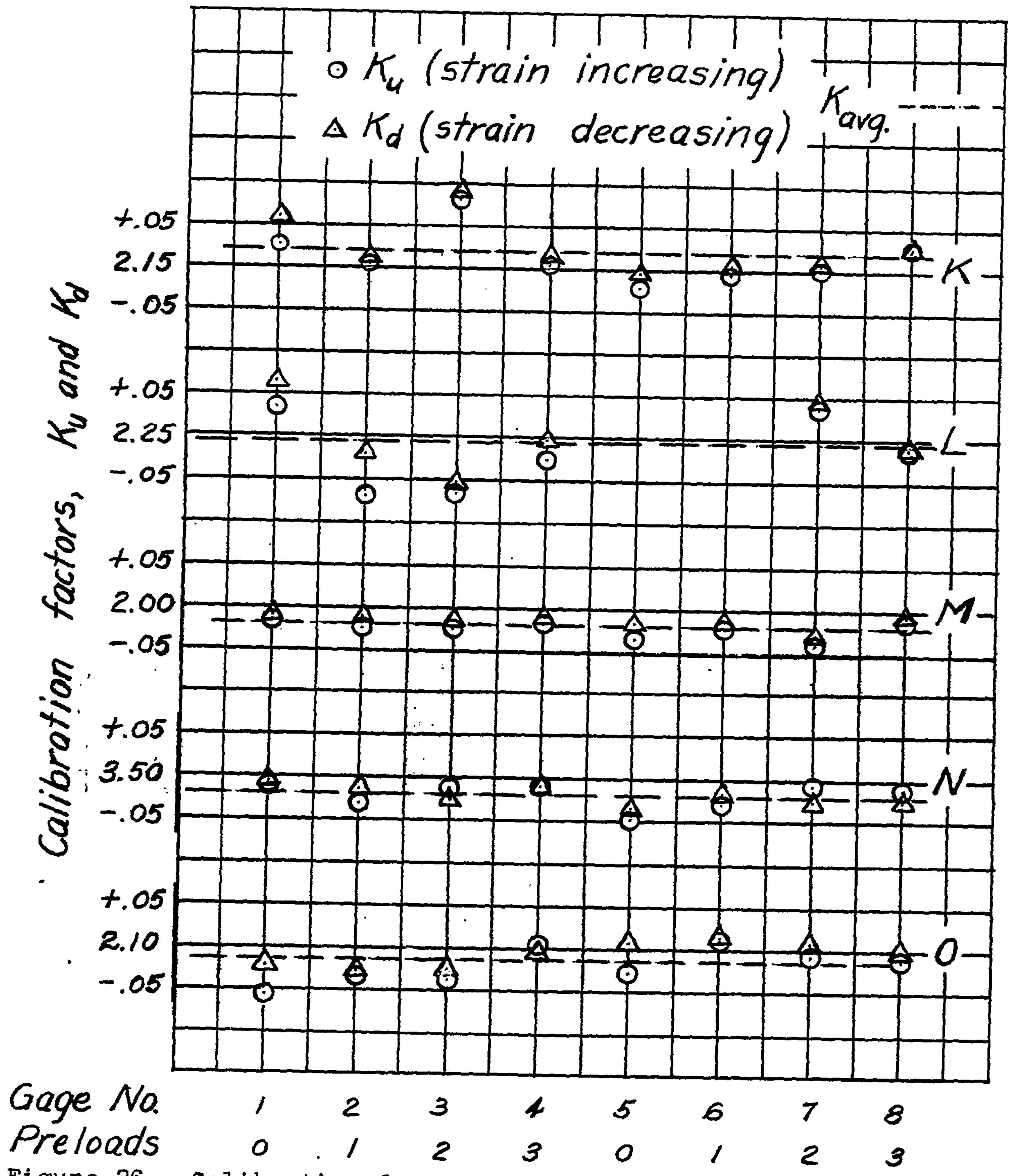

Figure 26.- Calibration factors vs. gage number and preloads (from table 1).